SPE 113890

Matrix-Fracture Transfer Function in Dual-Medium Flow Simulation: Review, Comparison, and Validation

Ahmad S. A. Abushaikha[1], SPE, and Olivier R. Gosselin, SPE, TOTAL S.A.

This paper was prepared for presentation at the 2008 SPE Europec/EAGE Annual Conference and Exhibition held in Rome, Italy, 9–12 June 2008.

Abstract

Most of porous naturally fractured reservoirs present a two-timescale flow-system, due to a two-scale heterogeneity which cannot be modelled explicitly, nor homogenised in reservoir simulation models. When the only flowing domain is the fracture network, and when the accumulation lies in porous and low permeable matrix blocks, the rate of exchanges between the two domains drives the recovery of such reservoirs. So called dual-porosity simulation models must incorporate an adequate transfer function between fracture and matrix in order to predict the recovery mechanisms for an optimal reservoir management. This is still true for dual-porosity / dual-permeability models, where the matrix domain is also flowing but at lower velocity.

During the past 40 years until recently several formulations have been proposed. In order to review, compare and validate some of them, this work first analyse the main recovery drivers in two-phase systems, like drainage and imbibition under capillary and gravity forces, on the basis of explicit (single-porosity) simulations of flows between fracture and a single matrix block on a fine mesh, characterised by the final value and the kinetics of the recovery. Varying the main dynamic parameters these simulations give a set of reference cases to benchmark the dual-medium models, like the classic Kazemi transfer function, the Quandalle-Sabathier one, and a new formulation recently proposed by Blunt et al. These dual porosity single-block transfer functions are easily discretised in time and coded.

The main findings are the disqualification of Kazemi formula, even with a gravity term, to represent any mechanism where the gravity is not negligible, especially in mixed-wet water-oil systems. Quandalle-Sabathier and Blunt transfer functions perform better, but the gravity forces remain difficult to be captured. The two first transfer functions are available in some commercial flow simulators, and their results on the same set of cases are consistent.

Introduction

Representing the correct behaviour of recovery mechanisms in naturally fractured reservoir in flow simulators is a challenging task. For a large class of fractured reservoirs, especially for multiphase production mechanisms, the standard (single-medium) numerical simulators cannot capture the two-scale heterogeneity, and the two-timescale flow behaviour. The dual-medium approach, using a transfer function (TF) to represent the exchange term between fracture (flowing domain) and matrix (stagnant domain) is a possible answer. It has been attempting with some success, since its introduction in the ‘60s by Barenblatt et al (Barenblatt, 1960), to accurately simulate this dual behaviour, and produce results accurate enough, and close to what fine-grid simulations would give. Nevertheless, it provides a practical solution because data requirement is substantially less and the speed of computation is much greater (Ramirez et al, 2007).

In this paper, we will give a brief history of the transfer function evolution over the past forty years. The two most common transfer functions have been developed by Kazemi and Gilman (1976-1986) on the one hand, and by Quandalle and Sabathier (1988-1990) on the other. They are generally available in commercial flow simulators. They assume two media (fracture and matrix) that are overlapped and the equations of motion and conservation of mass are written independently for each. The

[1] Now with Qatar Petroleum

transfer of fluid between the two media is accounted for by a source/sink term in the continuity equation; a semi-steady state approach is assumed.

The scope of this paper is as follows: focusing on the exchanges between fracture and matrix, when a single matrix block is surrounded by a large fracture, in simple black-oil systems (Water-Oil, Gas-Oil and Gas-Water), reviewing the main sensitive parameters, through fine grid explicit simulations, investigating and analyzing the two transfer functions mentioned above, and commonly used, plus a novel approach proposed by Blunt et al (Imperial College London), called the General Transfer Function (GTF), comparing their performances through simple time-discretised simulations (dual-medium, zero-dimension), against the fine grid reference cases (single-medium, three-dimension), discussing the drawbacks of each TF, and why they do not represent the recovery accurately. Finally we look at the options and results given by two commercial simulators.

Other important features of dual-medium modelling and simulation are outside the scope of this study, like calculation of effective fracture network permeability tensor (Garcia, 2007), the effective block size computation needed to define the static shape factors, the capillary continuity issue, and any thermal or compositional aspects.

Literature review

The transfer function and the so-called dual-porosity concept were formulated initially by Barenblatt et al (1960) under the continuum method approach, the base of most transfer functions today. Warren and Root (1963) disseminated this approach to the oil and gas industry worldwide, using single phase flow and pseudo steady state assumptions.

$$T = \sigma \frac{K}{\mu}\left(P^m - P^f\right) \qquad \text{(Eq. 1)}$$

Where, T is the transfer function (1/sec), σ the shape factor (1/cm^2), K the matrix permeability (mD), μ the viscosity (Pa.s), and P the pressure (atm); *m* stands for matrix and *f* for fracture.

Five main recovery mechanisms are involved in the transfer of fluid between matrix blocks and fractures: fluid expansion, viscous forces, capillarity, gravity and diffusion. Warren and Root model only included expansion. Multi-phase flow was extended into the model by Kazemi et al (1976), which used a different shape factor than Warren and Root; it was derived by a material balance on a cubic matrix block under the pseudo steady state assumption.

$$T_\alpha = \sigma \frac{K \cdot kr_\alpha}{\mu_\alpha}\left(P_\alpha^m - P_\alpha^f\right) \qquad \text{(Eq. 2)}$$

(Eq. 2) is the extension of (Eq. 1) to multi-phase flows with α referring to the phase and *kr* the relative permeability.

Gilman and Kazemi (1983); Gilman (1986) continued improving their model by adding a gravity term, and making it saturation dependent (see also Sonier et al., 1988). However, it was added to all the six matrix faces, which overestimates the speed of recovery, when gravity is the dominant mechanism. Quandalle and Sabathier (1989) corrected it by separating the horizontal and vertical flows. They also added viscous recovery term and tuning parameters.

Coats (1989) extended the dual-porosity model to compositional simulations, and derived another expression of the shape factor.

The pseudo-steady state assumption in the Warren and Root based transfer function (WRTF) created two main problems in simulating the recovery: (a) underestimate the speed of the recovery during early time; (b) mismatch the final recovery in gravity drainage recovery system, which is solved using integrated pseudo capillary pressure curve (see further discussion).

Lim and Aziz (1995) attempted to eliminate the pseudo steady state assumption by deriving a shape factor for single phase flow that depends on the analytical solution of single phase pressure-diffusion equation (Eq.3). However, during the derivation process an exponential approximation was used which made the solution during the early time not accurate.

$$\sigma = \frac{\pi^2}{\left(k_x k_y k_z\right)^{1/3}}\left(\frac{k_x}{l_x^2} + \frac{k_y}{l_y^2} + \frac{k_z}{l_z^2}\right) \qquad \text{(Eq. 3)}$$

Change (1993) also derived a shape factor that was time depended in 1D. However it was too complicated to implement in simulators. Dicretization of the matrix block has been researched and implemented by many authors. Gilman (1986) and

Ishimoto (1988) have used a sub-domain technique, which solved the pseudo-steady state assumption and allowed for the creation of saturation fronts. However it comes with a computational cost and some instability.

Counter-current imbibition processes have been recently addressed in modelling imbibition recovery mechanisms in fractured reservoirs. Chen et al (1995) have considered it to model early and late time in the matrix block. Di Donato et al. (2005), Lu et al. (2006) followed up this study, devised and proposed a new original TF in modelling the capillary imbibition They adapted their TF called 'Generalised Transfer Function' (GTF) for mixed-wet systems, inspired by the Quandalle and Sabathier approach, and originally merged with the GTF (Lu et al., 2007). In this paper we will address this non Warren&Root-based TF, which gives up focusing on the geometric (static) shape factor, but aimes to reproduce both early and late time of the recovery process. In their two papers, Lu et al. (2006, 2007) compared the performances of the GTF against the Kazemi-like TF, but not against the Quandalle and Sabathier. We will not analyse the most recent version of the GTF, which addresses the gravity effect more accurately (Lu, 2008).

Researchers have taken the transfer function from the well testing literature in the 1960s and have continued to improve it. Two phase, gravity, expansion, viscous and diffusion have been implemented. Time dependent shape factors and discretised matrix have been developed. However, simplicity and feasibility continue to be more dominating when trying to implement them in commercial simulators. The WRTFs continue to be used in commercial simulators. In this paper, we test two WRTFs and the GTF against different scenarios to understand the limits of each, and give recommendations.

Description of Reference Cases

Our reference cases, for water-oil (WO), gas-oil (GO) and gas-water (GW) systems, are the result of a three dimensional single-porosity fine grid model, which simulates the production of hydrocarbons stored in a single parallelipipedic matrix block, into the surrounding fracture. We define a base case (see appendix A), and investigate the sensitivity to the following parameters: shape of the matrix block (aspect ratio), block height, maximum capillary pressure value, density difference, wettability, number of fractures open to flow. This choice is no arbitrary, as the mechanisms of production are well known, i.e. mainly the competition between gravity and capillary forces. The gravity forces tend to push the oil outside the matrix while the water (or gas) is penetrating the matrix coming from the fracture. The same is observed when the matrix is saturated with gas and surrounded by fractures full of water. This mechanism is facilitated by capillary forces when (and while) the rock is water wet (WO system), and in the opposite, impeded by capillary forces when (and as soon as) the rock is hydrocarbon wet (oil-wet case, or gas every time). As a consequence the interaction between the parameters is also well known, like the balance between gravity and capillary forces, which depends on the ratio $(\Delta\rho.g.h / Pc)$, where $\Delta\rho$ is the density difference, h the height above the zero-capillarity plane, and Pc the capillary pressure.

The consequences are two-fold: the maximum micro-recovery is reached or not (governed by the hydrocarbon phase wet part of the capillary pressure curve), and it speeds up or slows down the recovery. In the following section the recovery profiles (in our cases equivalent to matrix saturation profiles) are given with respect to time (logarithmic x-axis).

A geometrical factor which partially governs the flow behaviour is the measure of possible exchanges, which depend on the area where fluids on both sides of the two domains (fracture and matrix) are in contact and in communication (open interface). This measure is given by the so-called shape factor. We already mentioned the basic definition of shape factor after Warren & Root, and more importantly for transfer function definition after Kazemi (Eq. 2). A more general and accurate definition of σ is given by Zhang et al. (1996), still as the inverse of the square of a characteristic length (L):

$$\sigma = L_c^{-2} = \frac{1}{V}\sum_{j=1}^{n}\frac{A_i}{l_j} \qquad \text{(Eq. 4)}$$

where V is the matrix block volume, and in each of the n possible flow direction j (according to the geometry of the block), A_i is the area open to flow, and l_i the distance between the no-flux boundary and the open surface. In the following section, we use this definition to characterise the capacity of exchange between matrix and fracture.

If the matrix block is parallelipipedic with block sizes l_x, l_y and l_z, and all 6 faces open, (Eq. 4) gives us the standard Kazemi shape factor:

$$\sigma = \frac{1}{4}\left(\frac{1}{l_x^{\,2}} + \frac{1}{l_y^{\,2}} + \frac{1}{l_z^{\,2}}\right) \qquad \text{(Eq. 5)}$$

The limitation of this paper prevents us to give the whole range of sensitivity runs (table in appendix B), so we only present the following cases.

Change in Matrix Shape (constant volume) - All systems
  - Shape A: 223.5 x 223.5 x 100 cm.
  - Shape B: 79.0 x 79.0 x 800 cm.
- Change in wettability - WO
- Change in Capillary Pressure - GO
  - Pc_Max value.
- Fluid density difference variation - WO
- Number of open fractures - All systems.

The matrix was surrounded by a large fracture (open or not across the 6 faces). Constant fracture fluid saturation and pressure were taken as boundary conditions. There was no fracture capillary pressure and the matrix relative permeability curves were not changed when the matrix capillary pressure was changed (changes of wettability or change of maximum Pc values).

The base case has been chosen with a mixed wettability for WO, oil wet for GO and water wet for GW. We chose a mixed wet system in WO, which is a more complex case, to extensively test fluid flow behaviour when capillary and gravity are working together and against each other (water wet case exhibits a more regular recovery curve, gravity and capillary acting always together).

The number of open fractures means we simulate one-, two- or three-dimensional flows, and this parameter has an impact on the shape-factor.

In the following section, 'Imbibition', respectively 'Drainage', refers to the wetting phase saturation increase, respectively decrease, in the matrix. However we still use the word 'imbibition' when water saturation is increasing, even though if water is not the wetting phase anymore (for instance when the wettability switches from water-wet to oil-wet).

The reference cases are simulated using standard (single-porosity) commercial flow simulators on a fine 3D grid where matrix block and surrounded fractures are explicitly represented (we used both Eclipse and Athos, and they gave the same results). The size of the mesh was chosen, by decreasing it until the results do not change significantly.

Table 1 lists the varied properties in each selected reference case. Table 2-5 in Appendix A lists the properties of the base case of each system. Unless said otherwise, the parameters are setup as they are in the base case.

System	WO, GO and GW		WO	GO
Parameter/ Reference case	Shape A	Shape B	$100<\Delta\rho_{ow}<500$	Pcgo_Max
Water Saturation @ Pc = $\Delta\rho_{ow}gh$ (WO only)	0.57	0.7	0.61, 0.73	-
Oil Density at initial matrix pressure (g/cm3)	0.65	0.65	0.91, 0.65, 0.51	0.65
Fracture Faces open to flow with matrix	1,2,3,4,6	1,2,3,4,6	6	6
Block width-x (cm)	223.5	79	79	79
Block length-y (cm)	223.5	79	79	79
Block height-z (cm)	100	800	800	800
Max Capillary Pressure @ Sg =1.0 (atm) (GO only)	1	1	-	0.1

Table 1: Reference cases 1, Sensitivity to number of fractures for shape A (WO system)

For the variation of shape factor cases (Ref. Cases 1 and 2), are as follows:

Faces open to flow with matrix		Shape factor (shape A)	Shape factor (shape B)
1S:	1 side	0.20	1.60
2S:	2 sides	0.80	6.41
4S:	4 sides	1.60	12.82
T&B:	Top and bottom	4.00	6.25E-2
2S_B:	2 sides, and bottom	1.80	6.42
2S_T:	2 sides, and top	1.80	6.42
1S_T&B:	1 side, top and bottom	4.20	6.47
2S_T&B:	2 sides, top and bottom	4.80	6.47
6F:	All 6 faces	5.60	12.88

Table 2: Variation of number of fractures for shape A and B, and shape factors (WO system)

Sensitivity Analysis

In this section, we selected some of the sensitivity runs, for each system, with respect to the parameters mentioned before. We also varies for some reference cases, the the number of fractures open to flows with the matrix. The observed features are listed in each case. At the end of this section we will summarise the observation for each system.

Water-Oil system

The production mechanism is here imbibition under always favourable gravity forces, and with the help of capillary forces when the matrix is water wet, but with the opposition of these later when the wettability switches to oil-wet.

Effect of Shape Variation

Ref. Case 1 (Shape A): Fig. 1 shows that, as the shape factor increases, due to the increase of communication to open fractures, the speed of recovery increases.

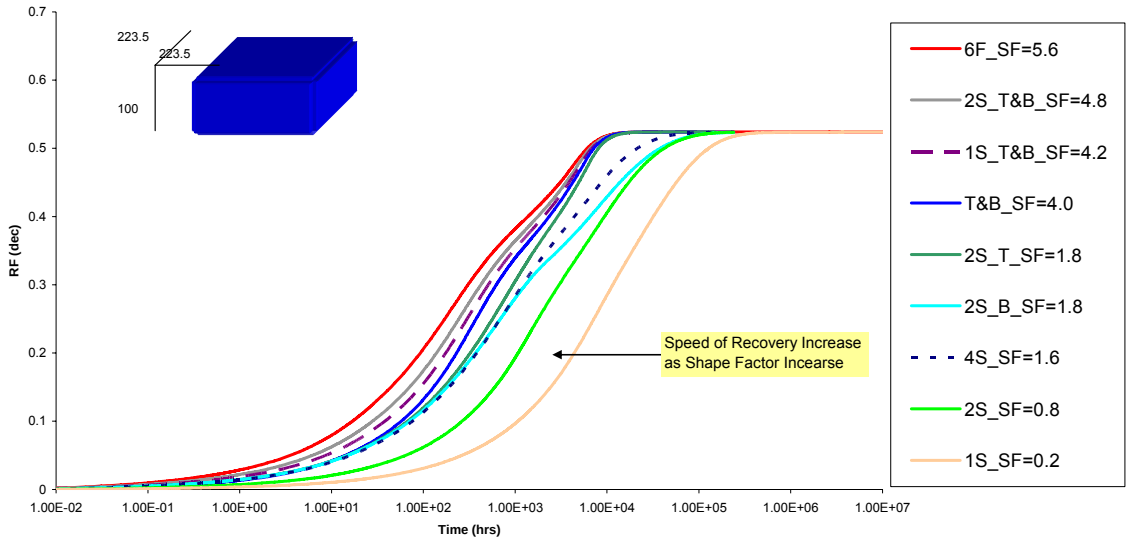

Figure 1: Ref. case 1, Sensitivity to number of fractures for shape A (WO system)

Ref. Case 2 (Shape B): Fig. 2 shows three effects:

- The shape factor strongly affects the speed of capillary imbibition reinforcing the gravity effect
- However it is not the case during the second phase of gravity imbibition, when capillary forces act against the gravity.
- The final recovery is larger than shape A because the matrix height is larger which will increase the equilibrium point between the gravity and capillary recoveries.

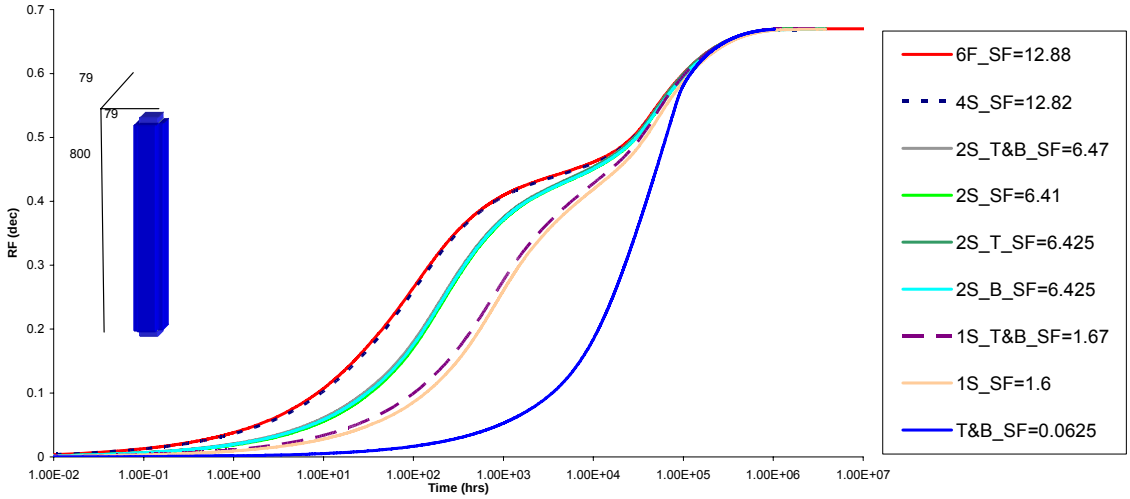

Figure 2: Ref. Case 2, Sensitivity to number of fractures for shape B (WO system)

Fluids Density Difference - 100 kg/m^3< $\Delta\rho_{ow}$ <500 kg/m^3

Ref. Case 3: As shown in Fig. 3, the final recovery for a difference of density of 100 kg.m^{-3}, is smaller than the base case ($\Delta\rho$ = 360 kg.m^{-3}). Block height and Pc curve being unchanged, the gravity forces are weaker. The opposite effect is observed for the density difference of 500 kg.m^{-3}.

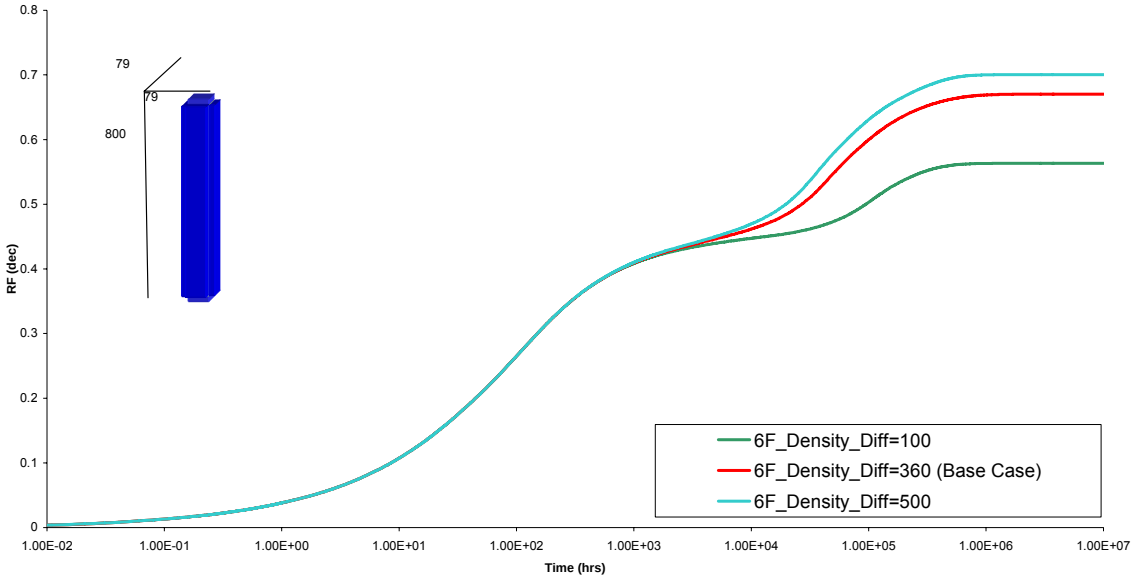

Figure 3: Ref. Case 3, Sensitivity to density difference, for 6 open fractures, and shape B (WO system)

Strength of water wettability – 0.3 < Sw @ Pc=0 <0.7

Ref. Case 4: As shown in Fig. 4, the final recovery for a less water wettability Pc(0.3)=0, is smaller than the base case (Pc(0.5)=0). Block height and fluid density being unchanged, the capillary force is weaker. The opposite effect is observed for the Pc(0.70)=0.

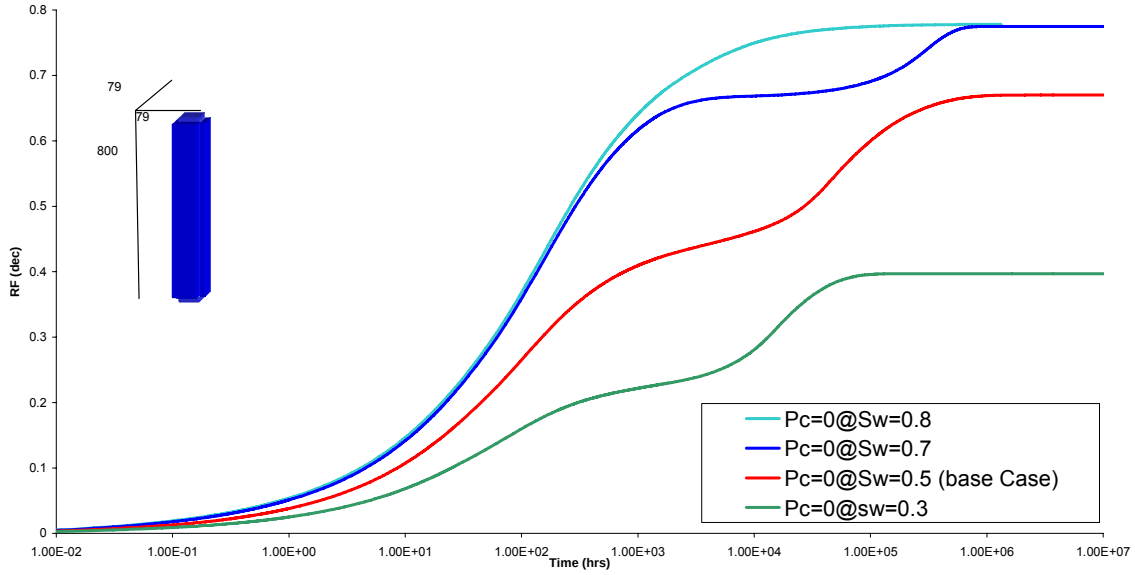

Figure 4: Ref. Case 4, Sensitivity to Sw(Pc=0), for 6 open fractures, and shape B (WO system)

Gas-Oil system

The production mechanism is drainage under the positive gravity forces, and in opposition with the negative capillary forces (never gas-wet).

Effect of Shape Variation

Ref. Case 5 (Shape A): Illustrated by Fig. 5, as the shape factor increases the speed of recovery increases, for the same reasons than the WO case.

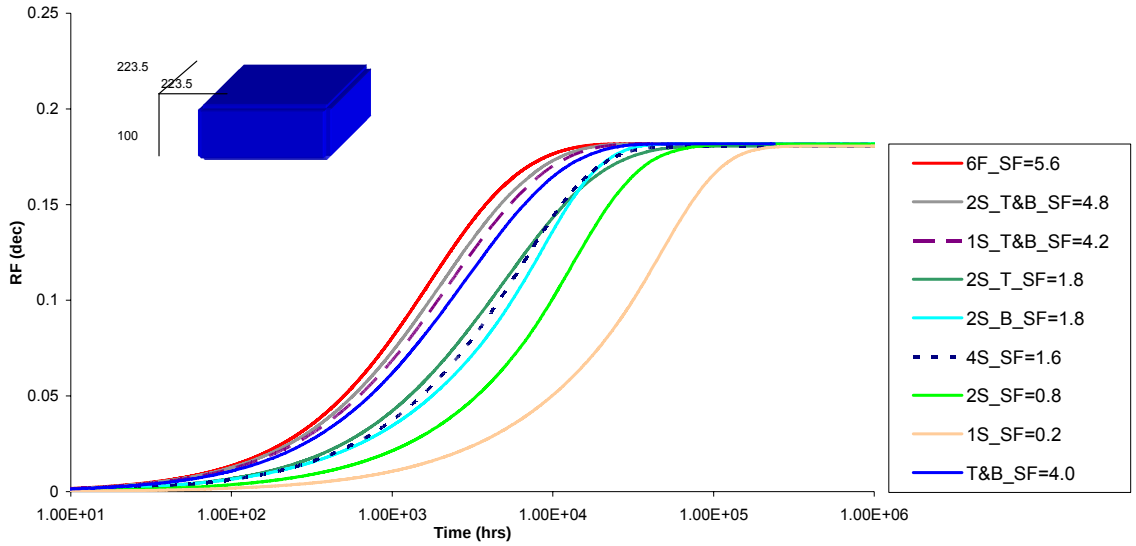

Figure 5: Ref. Case 5, Sensitivity to number of open fractures for shape A (GO system)

Ref. Case 6 (Shape B): the speed of gravity drainage is not largely affected by the variation of the shape factor, because the block length is larger than the horizontal sizes, and so the gravity is largely dominant, over the capillary forces opposed to the recovery (Fig. 6).

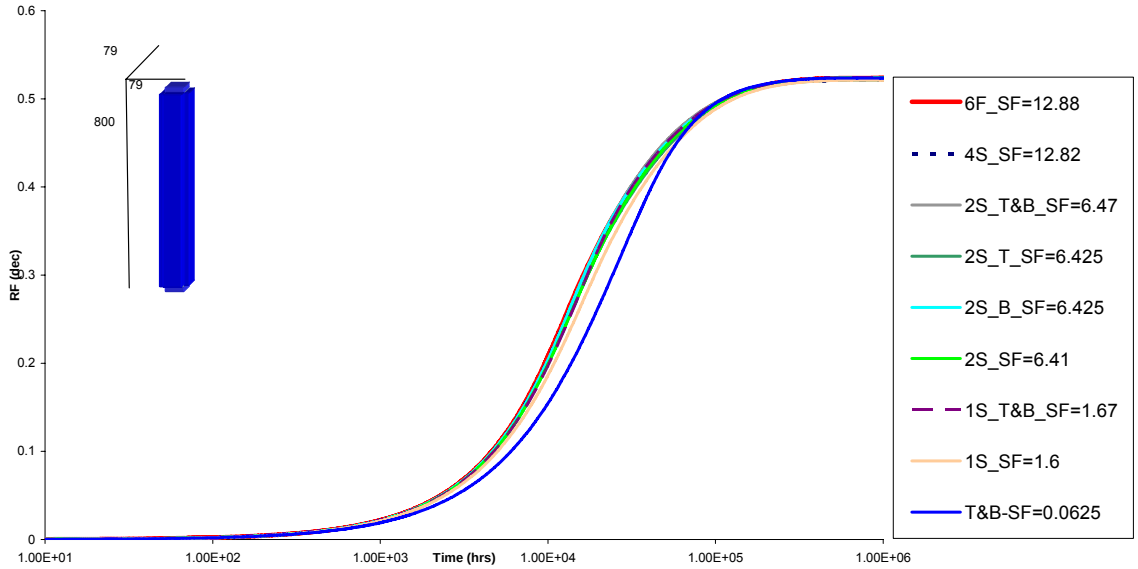

Figure 6: Ref. Case 6, Sensitivity to number of open fractures for shape B (GO system)

Capillary Pressure (Pc_Max_value= 0.1 atm)

Ref. case 7: Fig. 7 exhibits mainly a difference of final recovery which depends on capillary pressure value at Sor. It decreases as the maximum Pc increases (impact on the equilibrium point given by $(\Delta\rho.g.h / Pc)$.

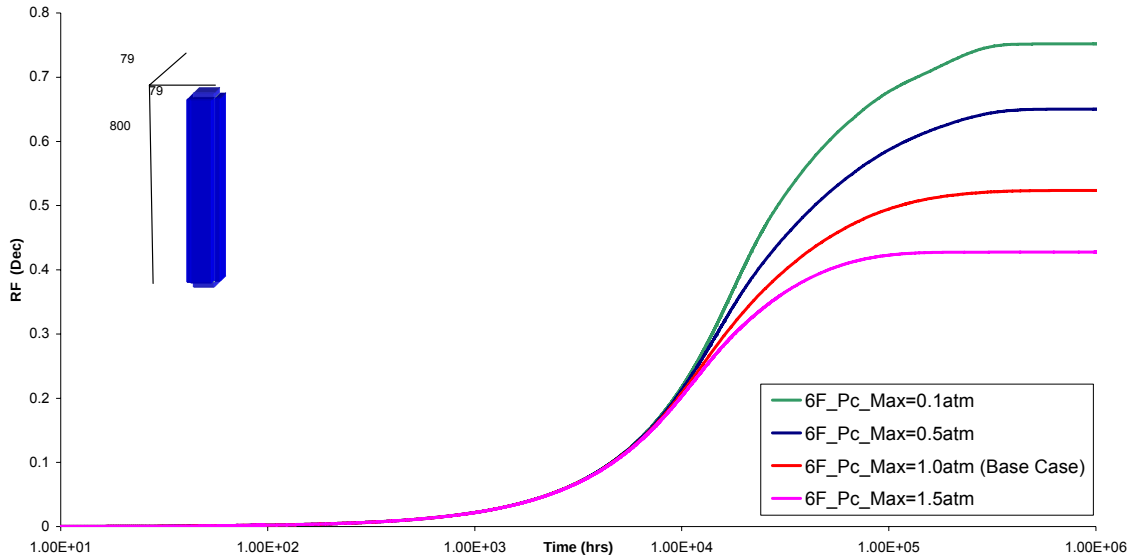

Figure 7: Ref. Cases 7, Sensitivity to number of fractures for shape B (GO system)

Gas-Water system

Effect of Shape Variation

Ref. Case 8 (Shape A): as the shape factor increases the speed of recovery increases, as already observed for WO system (Fig. 8).

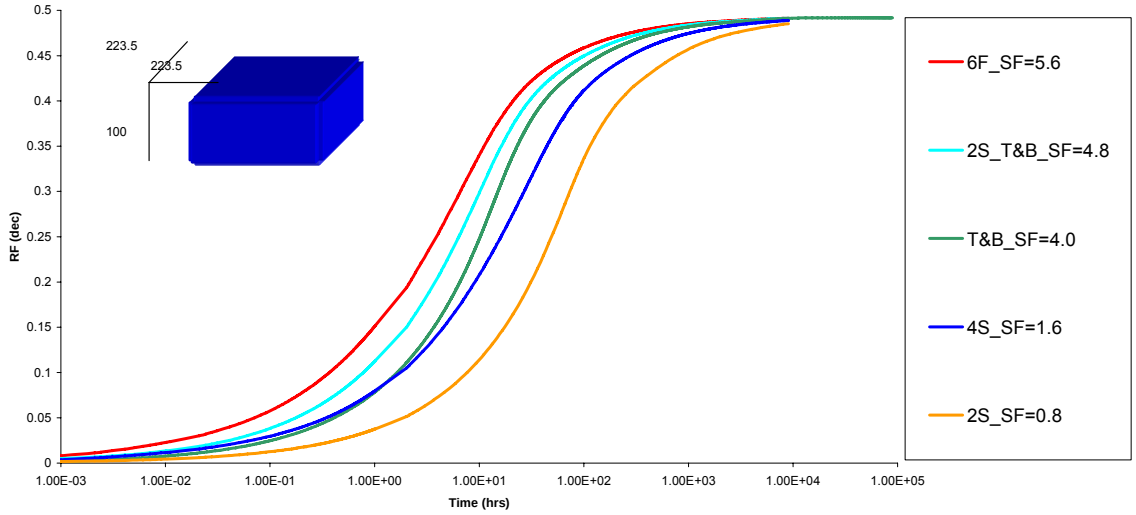

Figure 8: Ref. Case 8, Sensitivity to number of fractures for shape B (GW system)

Ref. Case 9 (Shape B): as the shape factor increases the speed of recovery increases as well (Fig. 9).

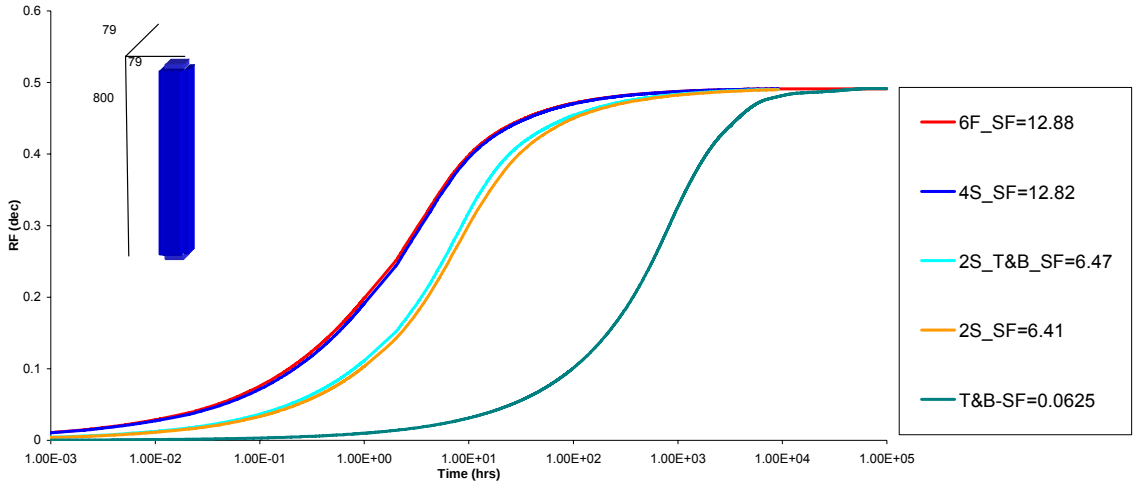

Figure 9: Ref. Case 9, Sensitivity to number of fractures for shape B (GW system)

Summary of the main features

From the previous sensitivity analysis we observed some features in each system, which are listed below.

Water-Oil system
- As the shape factor increases the speed of recovery increases.
- The final recovery depends on fluid density, matrix height and capillary pressure.
- The speed of recovery during the gravity imbibition does not strongly depend on the shape factor as long as the matrix height is much larger than the sides.
- Regular when the matrix is water wet, the recovery curve presents a typical double-hump shape in case of mixed wettability

Gas-Oil system
- The speed of recovery during the gravity drainage does not strongly depend on the shape factor as long as the matrix height is much larger than the sides.
- The final recovery depends on fluid density, matrix height and capillary pressure.

Water-Gas system
- As the shape factor increases the speed of recovery increases.

Dual-medium numerical models

The concept of dual-medium model leads to double the usual flow equations (mass and momentum conservation) everywhere over the field, to represent the two domains (stagnant and flowing) present at the same position, each with its owns property coefficients, and to add a transfer term (of opposite signs) in both systems of equation, as a sink term (like wells). If the stagnant domain (matrix one for instance) has only communication with the flowing one (e.g. fracture network), the former domain equation is reduced to the mass balance equation (so called dual porosity, instead of dual permeability model). This conceptual model is not physical in its continuous expression, but when discretised, represents a upscaling compromise between a standard model with homogenised properties, and a standard finely-gridded model, taking into account all heterogeneities (only realistic for large scale features, or for a reduced domain). The core of this representation is the transfer function formulation.

Equations

For each domain (d=f, m), and each component, or Black Oil pseudo-component (ξ), the mass conservation can be written (if we omit the well sink term) as:

$$\frac{\partial}{\partial t}\left(\sum_{\alpha=o,w,g} M^{d}_{\xi,\alpha}\right)+\sum_{\alpha=o,w,g}\nabla\cdot\left(\rho_{\alpha}c_{\xi,\alpha}u_{\alpha}\right)=\pm\Gamma_{\xi}=\sum\rho_{\alpha}c_{\xi,\alpha}T_{\alpha} \qquad \text{(Eq. 6)}$$

where α is the phase (o=oil, w=water, or g=gas), ρ the phase density, c the concentration, u the Darcy phase velocity, and M the mass of component ξ within the phase α.

$$M^{d}_{\xi,\alpha} = \phi^{d} \rho_{\alpha} S^{d}_{\alpha} c_{\xi,\alpha} \quad \text{(Eq. 7)}$$

and Γ is the mass transfer term for the component ξ, T_α the volume transfer term within the phase α.

The Transfer Functions

We briefly recap below the bases of three WRTFs, and present one novel and original transfer function suggested by M. Blunt, H. Lu and al. (GTF for Generalised Transfer Function).

KZ: Kazemi et al. (1976)

The Kazemi model is an extension of the single-phase flow equation derived by Warren-Root which are based on the assumption the flow towards the well bore takes place in the fracture network and the matrix feeds the system with the stored hydrocarbons under semi-steady state flow conditions; neglecting the early time effect. The transfer function is a conservation of momentum function based on Darcy's law. It takes into account three recovery mechanisms; expansion, capillary and gravity. For a simple dead oil case (confusion between component ξ and phase α), we get:

$$T_\alpha = 4\left(\frac{1}{l_x^2}+\frac{1}{l_y^2}+\frac{1}{l_z^2}\right)\lambda_\alpha K_m\left(\Psi_\alpha^m - \Psi_\alpha^f\right) = \sigma\lambda_\alpha K_m\left(P_\alpha^m - P_\alpha^f\right) \quad \text{(Eq. 8)}$$

which is (Eq 2) with the shape factor defined by (Eq 5), Ψ being the potential $P - \rho \cdot g \cdot h$, but the phase density is the same in both domain, so the gravity term vanishes. A diffusion term is possible, but not given here.

G&K: Gilman and Kazemi (1983), Gilman (1986), Sonier et al. (1988) - Kazemi with gravity term

Gilman and Kazemi (1983) continued improving their model by making the gravity term saturation dependent (deriving the gravity from the potential difference, considering the matrix saturation, and the surrounding fracture saturation). Below are two equations; oil and water (still for a dead oil system):

$$T_o = 4\left(\frac{1}{l_x^2}+\frac{1}{l_y^2}+\frac{1}{l_z^2}\right)\frac{K_m kr_o}{\mu_o}\left(P_o^m - P_o^f + (\rho_w - \rho_o)(S_{wD}^f - S_{wD}^m)\frac{gh}{2}\right) \quad \text{(Eq. 9)}$$

$$T_w = 4\left(\frac{1}{l_x^2}+\frac{1}{l_y^2}+\frac{1}{l_z^2}\right)\frac{K_m kr_w}{\mu_w}\left(P_o^m - Pc_o^m - P_o^f + Pc_o^f - (\rho_w - \rho_o)(S_{wD}^f - S_{wD}^m)\frac{gh}{2}\right) \quad \text{(Eq. 10)}$$

The gravity model depends on the saturation height; the higher the matrix block the faster oil is recovered. It is calculated using:

$$S_{wD}^f = \frac{S_w^f - S_{wi}^f}{1 - S_{or}^f - S_{wi}^f} \quad \text{and} \quad S_{wD}^m = \frac{S_w^m - S_{wi}^m}{1 - S_{or}^m - S_{wi}^m} \quad \text{(Eq. 11)}$$

Where,

S_w^m, matrix water saturation; S_{or}^m, matrix residual oil saturation; S_{wi}^m, matrix initial water saturation (idem for the fracture. However, the gravity term is added to all of the six faces, which overestimates the speed of recovery.

Q&S: Quandalle and Sabathier (1989)

Quandalle and Sabathier (1989) corrected the estimation of the G&K TF, by separating the horizontal and vertical flows. They also added viscous recovery term and tuning parameters. This transfer function is also based on the Warren-Root semi-steady state flow model. It takes into account four recovery mechanisms; (expansion, capillary, gravity and viscous – diffusion not presented here) and the flow is defined on all the six faces of the block; each its property.

$$T_\alpha = \sum_{\substack{p=x^+,x^-,y^- \\ ,y^+,z^-,z^+}} \left[2\sigma_p \left(\frac{K_{m,p} kr_{\alpha,p}}{\mu_\alpha} \right)_p \left(\Psi^m_{\alpha,p} - \Psi^f_{\alpha,p} \right) \right] \quad \text{(Eq. 12)}$$

The details of the derivation are given in Appendix D, and that leads to the following expression:

$$\begin{aligned} T_\alpha = {} & \sigma\, \lambda_\alpha\, K_{m,hor} \left(P^m_\alpha - Pc^m_\alpha - P^f_\alpha + Pc^f_\alpha \right) \\ & + \sigma_{gd}\, K_{m,ver} \left\{ \begin{array}{l} \lambda_{\alpha,z+} \left(P^m_\alpha - Pc^m_\alpha - P^f_\alpha + Pc^f_\alpha + (\rho^f_\alpha - \rho^f_*) g \frac{l_z}{2} \right) \\ + \\ \lambda_{\alpha,z-} \left(P^m_\alpha - Pc^m_\alpha - P^f_\alpha + Pc^f_\alpha - (\rho^f_\alpha - \rho^f_*) g \frac{l_z}{2} \right) \end{array} \right\} \end{aligned} \quad \text{(Eq. 13)}$$

where $\lambda = kr/\mu$ is the mobility, possibly directional in z direction, where two shape factor are needed:

$$\sigma = 4\left(\frac{1}{l_x^2} + \frac{1}{l_y^2} \right) \qquad \text{and} \qquad \sigma_{gd} = 2\left(\frac{1}{l_z^2} \right) \quad \text{(Eq. 14)}$$

GTF

The transfer function developed by Blunt et al (Lu et al;, 2006, 2007)) accounts for four recovery mechanisms; expansion, displacement (capillary and gravity), diffusion. Each mechanism is treated separately and then summed up. A Zimmerman et al (1993) term is added to account for the early time recovery of the fluids. In this paper we use their updated version (Lu et al., 2007) which separates the vertical and horizontal displacement, similar to Q&S.

$$\Gamma_\xi = \sum_{\alpha=o,w,g} \rho_\alpha c_{\xi,\alpha} \left(T_{e,\alpha} + \phi_m \sum_{q \neq \alpha} T_{s,\alpha\beta} \right) \quad \text{(Eq. 15)}$$

where the diffusion term is omitted, $\Gamma_{e,\alpha}$ is the fluid expansion term, and $\Gamma_{s,\alpha\beta}$ the fluid displacement term.

Fluid expansion

$$T_{e,\alpha} = \sigma K_m \lambda^m_\alpha \left(\psi^f_o - \psi^m_o \right) \frac{\left| \psi^f_o - \psi^m_{oi} \right| + \left| \psi^m_o - \psi^m_{oi} \right|}{2Max\left(\varepsilon \psi^m_o ; \left| \psi^m_o - \psi^m_{oi} \right| \right)} \quad \text{(Eq. 16)}$$

Fluid displacement (vertical and horizontal displacement)

$$T_{s,\alpha\beta} = T^V_{s,\alpha\beta} + T^H_{s,\alpha\beta} \quad \text{(Eq. 17)}$$

For water displacing oil or gas they use.

$$T^H_{s,w\beta} = \delta^H_{w\beta} \left(S^m_{wi} + F(S^f_w)(S^{m*H}_w - S^m_{wi}) - S^m_w \right) \frac{\left| S^{m*H}_w - S^m_{wi} \right| + \left| S^m_w - S^m_{wi} \right|}{2Max\left(\varepsilon S_{wm} ; S^m_w - S^m_{wi} \right)} \quad \text{(Eq. 18)}$$

$$T^V_{s,w\beta} = \delta^V_{w\beta} \left(S^m_{wi} + F(S^f_w)(S^{m*V}_w - S^m_{wi}) - S^m_w \right) \frac{\left| S^{m*V}_w - S^m_{wi} \right| + \left| S^m_w - S^m_{wi} \right|}{2Max\left(\varepsilon S_{wm} ; S^m_w - S^m_{wi} \right)} \quad \text{(Eq. 19)}$$

$$F(S) = \frac{1 - e^{-\sqrt{K_f / K_m} S}}{1 - e^{-\sqrt{K_f / K_m}}} \quad \text{(Eq. 20)}$$

$$\delta_{w\beta}^{V} = \frac{3\lambda_w^{m^*}\lambda_\beta^{m^*}}{\lambda_{tm}^{*}}\left(\frac{\varsigma_{w\beta}J^{*V}}{H^2}\sqrt{\frac{K_m}{\phi_m}} + \frac{K_m\left|\Delta\rho_{w\beta}\right|g}{\phi_m H}\right) \quad \text{and} \quad \delta_{w\beta}^{H} = \frac{3\lambda_w^{m^*}\lambda_\beta^{m^*}}{\lambda_{tm}^{*}}\left(\frac{\varsigma_{w\beta}J^{*H}}{L_c^{\,2}}\sqrt{\frac{K_m}{\phi_m}}\right) \qquad \text{(Eq. 21)}$$

The gravity and capillary are summed up to formulate the displacement term with no justification. This simplification could create some inconsistency in simulating the recovery.

A diffusion term (not multiplied by density and concentration) is also added, with the same Zimmerman formalism (Lu et al., 2006).

Pseudoisation: Integrated Pc curve

In WO, GO and WG systems, the gravity forces are always favourable to produce the hydrocarbons from the matrix block. The capillary forces are also favourable when the matrix rock is water-wet (in WO), or as far as the Pc is positive (WO, mixed-wet system). Thus the micro-recovery can only be reached, for water-wet system, or if there are no capillary forces, and is determined by the end points (S_{wi}, S_{or}, S_{gc}). If not, the final recovery is reached when the capillary pressure and the gravity pressure are in equilibrium, and there is trapped oil (WO, GO), or gas (GW), determined by the area between the P_c curve (negative part of imbibition curve for WO, or drainage curve for GO or GW) and the saturation axis, where the y-axis represent both P_c, and height (h)over/under the zero-capillary plane ($\Delta\rho.g.h = P_c$). Fig. 10 illustrates the case of a GO system.

However, the dual-medium simulators (based on G&K or Q&S) only deal with the capillary pressure value at the centre of the block and they assume it is homogenous for the block, Figure 19. So when equilibrium is reached there will be some miss representation of the residual oil. In order to correct for this behaviour the reservoir engineer (or the simulator) needs to calculate a new capillary pressure curve that estimates the right final recovery at equilibrium.

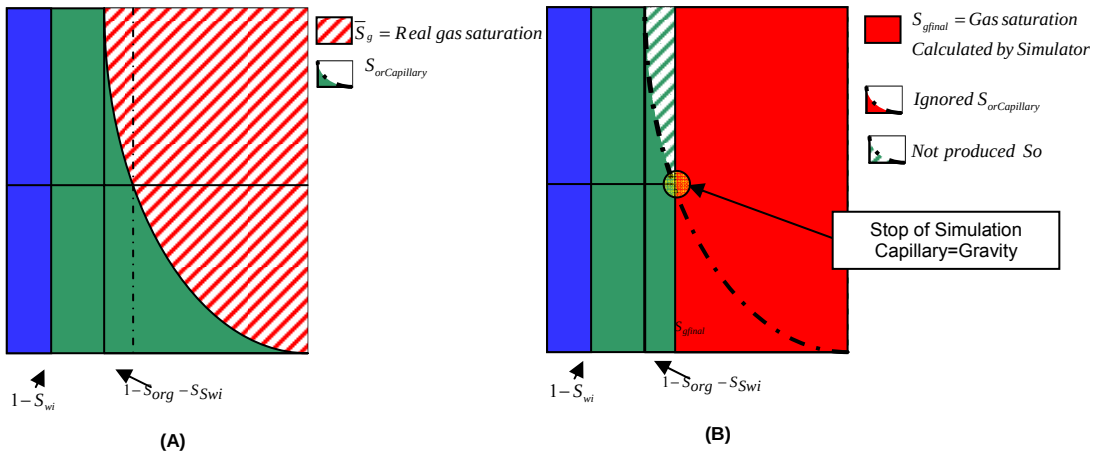

Figure 10, Gas-Oil Drainage (A) Fine grid Single-Porosity matrix block (B) Dual-Porosity matrix block

This is quite obvious for the Q&S formulation, for each P_c value (corresponding to a value of $h/2$) the corresponding saturation (S_{gfinal}) is increased until the red area equals the real hachured one. Using the G&K formulation requires a specific pseudoisation (not detailed here). The GTF formulation integrates this issue, because the correct final saturation, S^{*V}, is pre-calculated using (Eq. 22) and assigned in (Eq. 19) before the start of simulation. When S^{*V} is reached the fluid displacement equals zero and the fluid transfer due to capillary and gravity stops.

$$S_w^{*V} = \frac{1}{L}\int_0^L P_{cowm}^{-1}\left((\rho_w-\rho_o)gz\right)dz = \frac{a}{L}\ln\left(1+\frac{L}{2a}\right) \quad \text{where} \quad a = \frac{0.3\sigma_{ow}}{(\rho_w-\rho_o)g}\sqrt{\frac{\phi_m}{K_m}} \qquad \text{(Eq. 22)}$$

where a is a representative height of the transition zone (Lu et al.,2007):

Transfer function Performances vs reference solutions

In this section, we illustrate the observed features with sensitivity analysis, comparing each transfer function with the fine grid reference cases. The four transfer functions were tested using a simple zero-dimensional numerical model to compute the transfer rate between matrix and fracture. We could have chosen the dual-porosity commercial simulators to assess the TFs. However we preferred to decouple the problem: (a) assess the TF formulation coded by ourselves; (b) check if the commercial simulator available TFs actually give the results they are supposed to deliver. So we implemented in a spreadsheet the time

discretisation of these ordinary differential equations (any other tool or language would be suitable). We used the same parameters and boundary conditions than in the fine grid reference cases. An integrated capillary pressure curve was necessary to correct for the final recovery value in the KZ type and QS transfer functions (Cf. Pseudoisation section above). Kazemi with and without gravity is tested in Water-Oil system to show the importance of representing the gravity term in the Warren-Root based transfer functions.

Water-Oil system

Shape A (Fig. 11)

- *KZ:* the final recovery is mismatched because there is not gravity force to overcome the opposing capillary pressure.
- *G&K:* is slow during early recovery due to the semi-steady state assumption however the speed of recovery was not overestimated. Because the gravity effect is small; height is 100 cm.
- *Q&S:* is slower than the reference because of the semi-steady state assumption that excludes the early time recovery (Behaviour #1).
- *GTF:* gives the most accurate match however at the end of the capillary dominated recovery it stays at the same speed. This behaviour is caused by the constant value of delta factor.

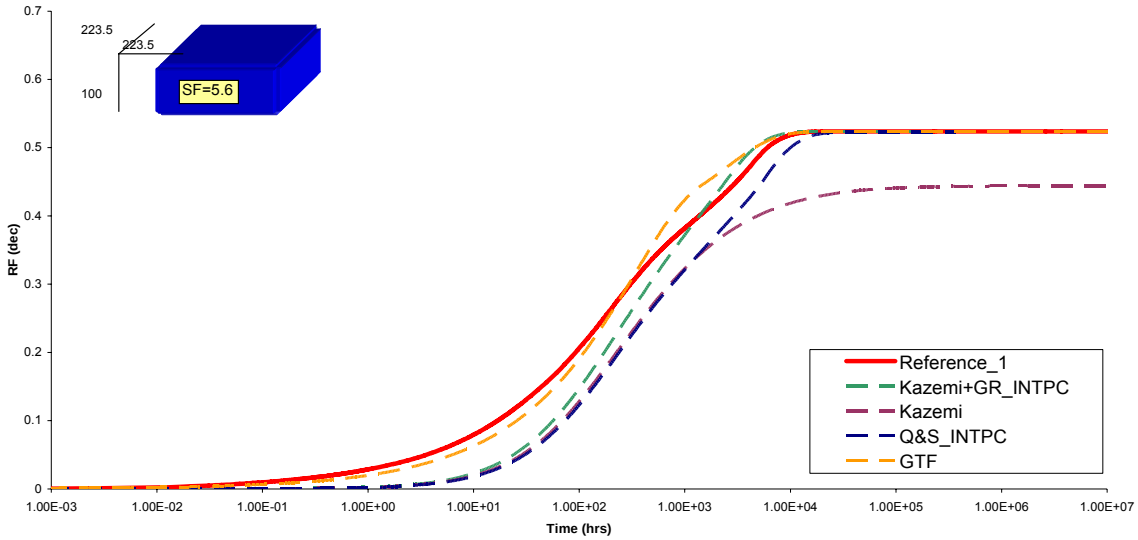

Figure 11: Ref. case 1, TF comparison, 6 open fractures for shape A (WO system)

Shape B (Fig. 12)

- *KZ, Q&S, GTF:* Similar to shape A.
- *G&K:* overestimates the speed of recovery because it accounts for the gravity in all the six directions.

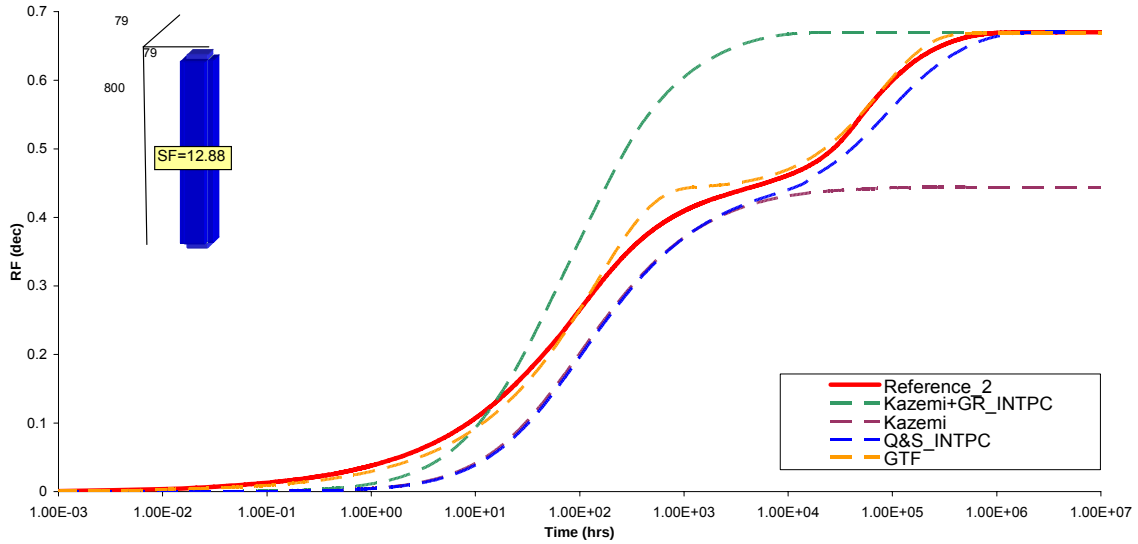

Figure 12: Ref. case 2, TF comparison, 6 open fractures for shape B (WO system)

Decrease in Matrix-Fracture Fluid Density Difference(Fig. 13)

Transfer functions showed the same behaviour as shape B with less final recovery.

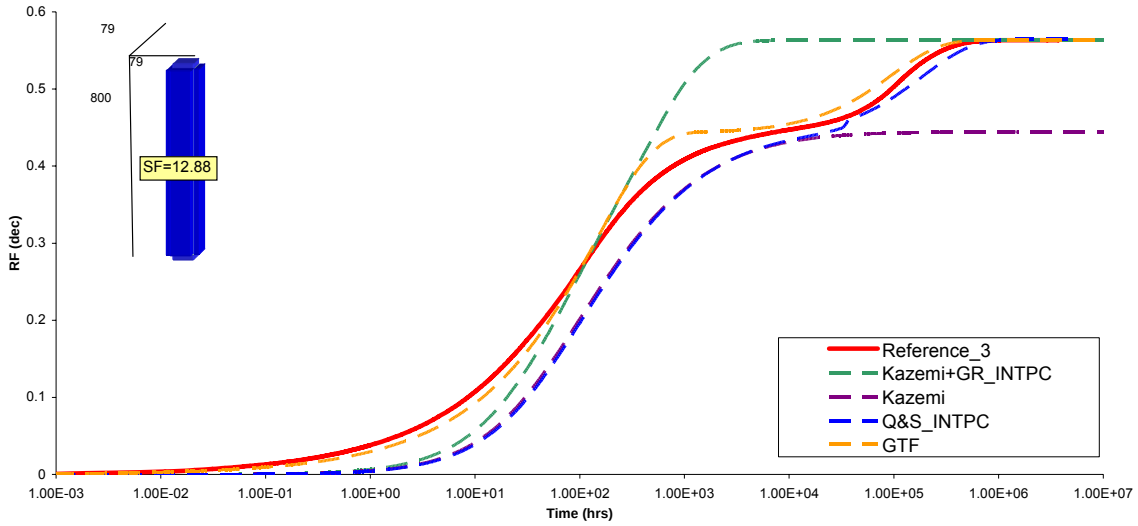

Figure 13: Ref. case 3, TF comparison, density difference= 100 kg/m^3, 6 open fractures for shape B (WO system)

Wettability (Shape B)

From the Ref. Cases 4, we keep the water-wet case, and the mixed-wet one (Pc=0 @ Sw=0.7), and compare the four TFs: Kazemi without gravity term (KZ), Kazemi with gravity term (G&K), Quandalle and Sabathier (Q&S), and the Lu et al (GTF).

Water-Wet case (Fig. 14)

- Since the capillary is the dominant recovery mechanism, Q&S and KZ are almost identical. It is not the case for G&K where the gravity is overestimated.
- For GTF: because the delta factor value is constant, the recovery will stay at the same momentum until the end. Nevertheless it is water saturation dependent, but delta still has a strong momentum.

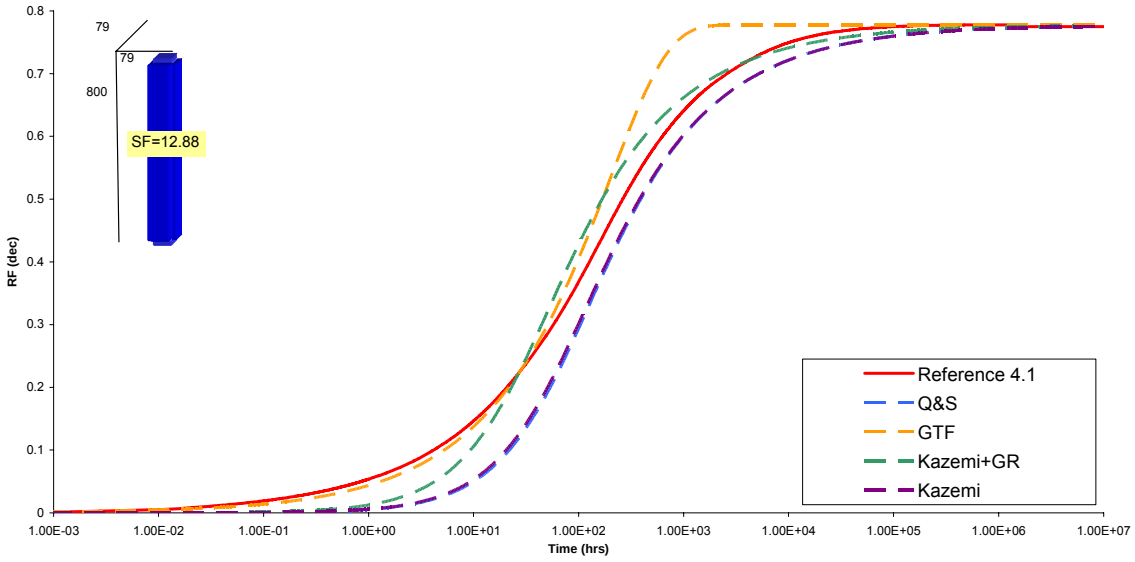

Figure 14: Ref. Case 4, TF comparison, Water-wet, for 6 open fractures, and shape B (WO system)

Mixed-Wet case – Pc=0 at Sw=0.7(Fig. 15)

- The same general observations are valid, until the late time.
- The typical late time behaviour of mixed-wet system (depending of the shape of Pc and the saturation point where the wettability switches from water to oil) is roughly represented by Q&S and GTF.
- G&K misses it completely.

- KZ cannot go further the point where Pc becomes negative (no gravity engine).

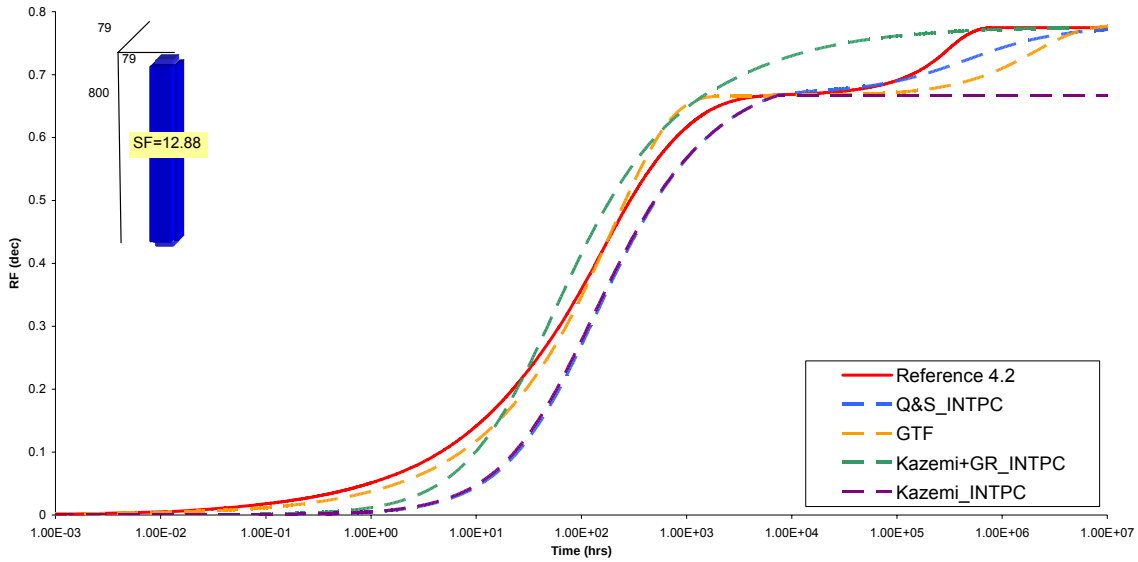

Figure 15: Ref. Case 4, TF comparison, mixed-wet, for 6 open fractures, and shape B (WO system)

Gas-Oil system

Shape A (Fig. 16)

- *G&K, Q&S and GTF:*: overestimated the speed of recovery.

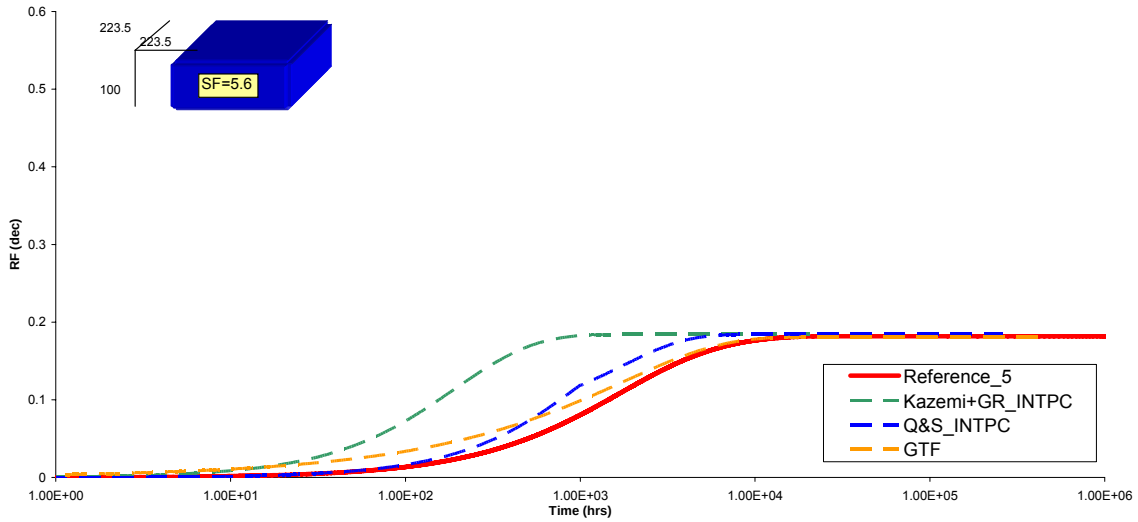

Figure 16: Ref. case 5, TF comparison, 6 open fractures for shape A (GO system)

Shape B (Fig. 17)

- *G&K:* overestimated the speed of recovery because it accounts for the gravity in all the six directions.
- *Q&S:* showed a good match during early recovery however got slower versus time (Behaviour #2).
- *GTF:* missed the kinetics.

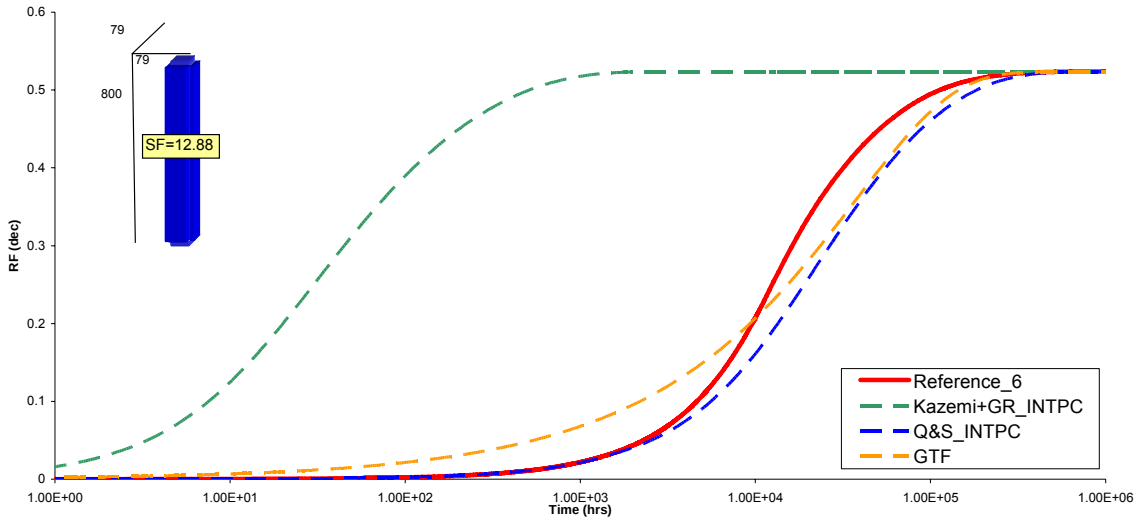

Figure 17: Ref. case 6, TF comparison, 6 open fractures for shape B (GO system)

Capillary Pressure (Fig. 18)

- *G&K and Q&S*: same behaviour as previous cases.
- *GTF:* missed the match because the mobility end points were taken very close to the fluid residuals which decreases delta (Behaviour #3).

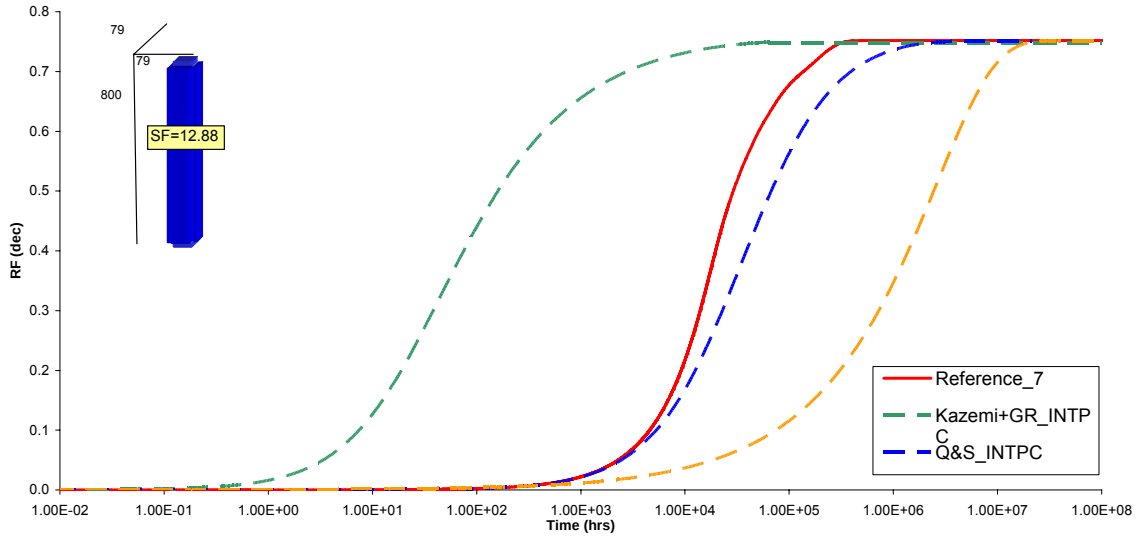

Figure 18: Ref. case 7, TF comparison, Pc_max=0.1 atm, 6 open fractures for shape B (GO system)

Water-Gas system

Shape A (Fig. 19)

- *G&K*: good match however slower during early time recovery and larger at the end of recovery (due the overestimation of gravity)
- *Q&S:* good match however slow at early time.
- *GTF:* good match however faster at the end of the recovery.

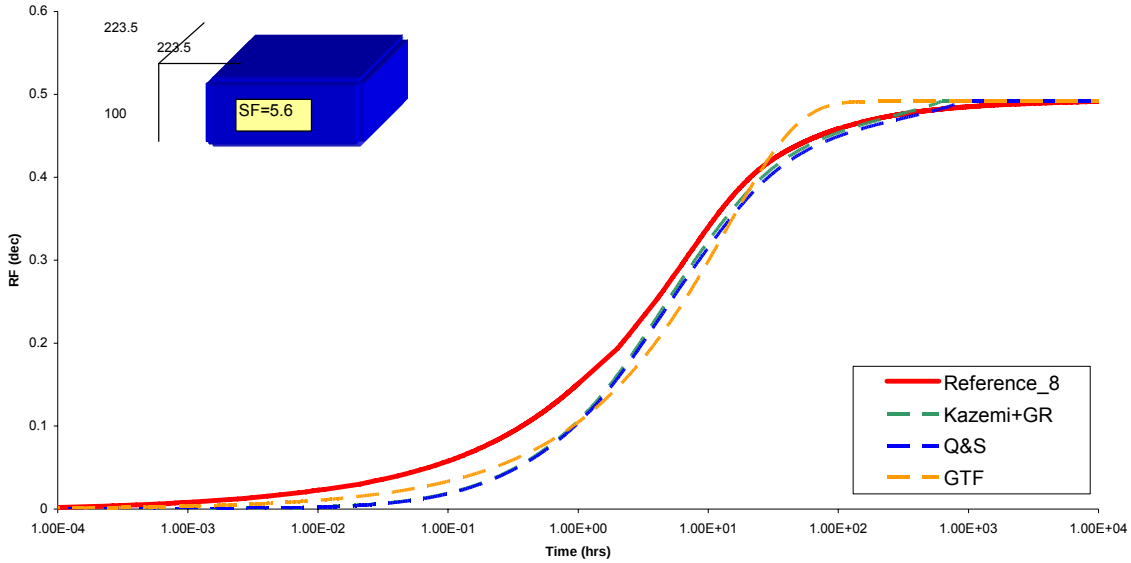

Figure 19: Ref. case 8, TF comparison, 6 open fractures for shape A (GW system)

Shape B (Fig. 20)

- *G&K:* good match however slower during early time recovery, then get faster than the reference case because of the gravity effect.
- *Q&S:* good match however slow at early time.
- *GTF:* good match however slow at early and fast at end.

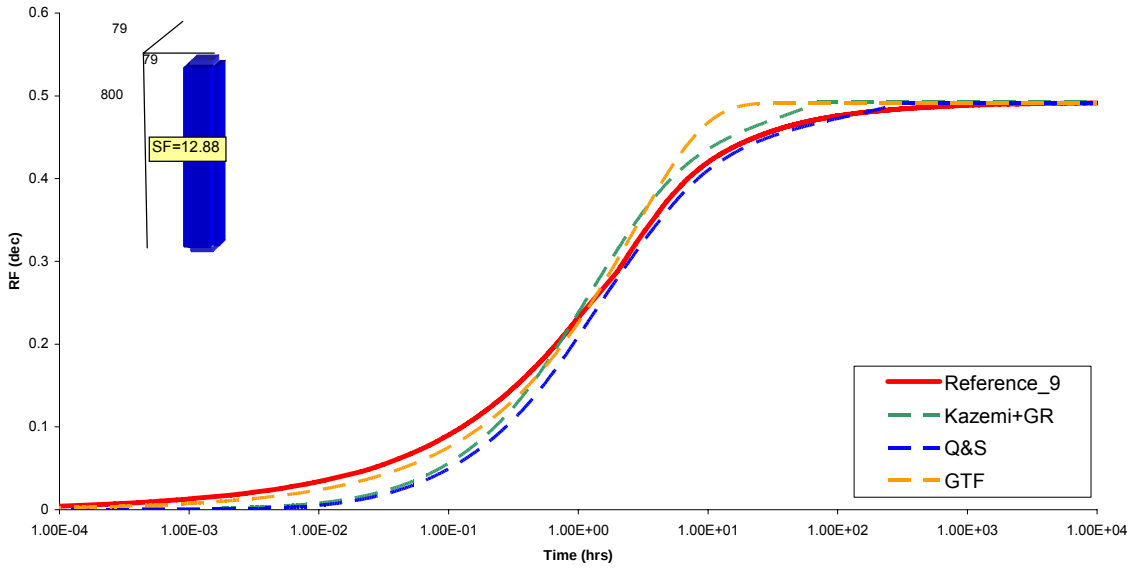

Figure 20: Ref. case 9, TF comparison, 6 open fractures for shape B (GW system)

Behaviour Analysis

Behaviour Number One: Why WRTFs do not simulate the speed of the early recovery as fast as the reference case in Water-Oil/Gas system with Pc?

Because they assume the saturation front reaches the centre of the block instantly at the beginning of the invasion by the fracture fluid under the semi-steady state assumption (Fig. 21-B). It is not the case in the reference solution where the saturation front takes the shape of the Pc curve and moves rapidly until it reaches the centre of the block (Fig. 21-A). This behaviour gives high kr_o and Pc values in the saturation front's path until the front reaches the centre. This promotes higher speed of recovery in the early time which ends at this matrix saturation value (Eq. 23). The WRTF do not simulate this recovery behaviour thus they miss the speed of early time recovery.

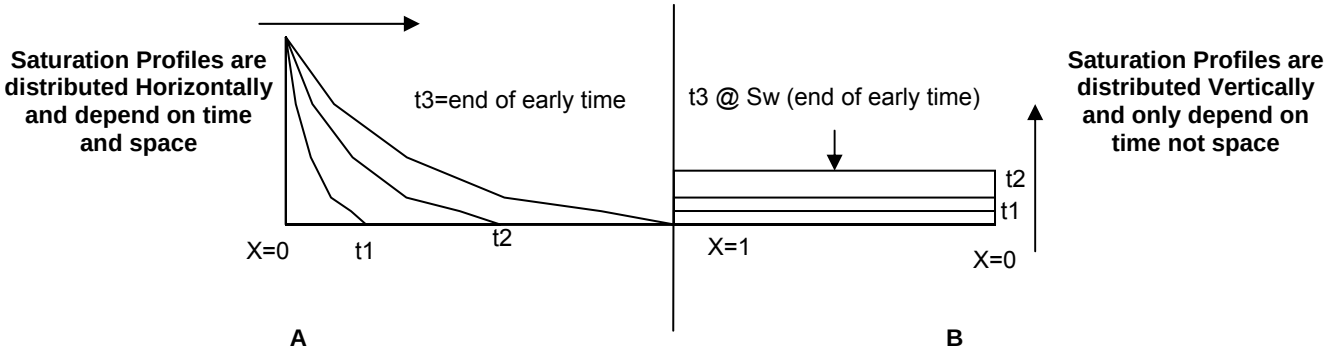

Figure 21, Saturation Profiles for (A) Fine grid single porosity and (B) dual-porosity

$$Sw(t = end\ early\ time) = \int_0^1 \frac{Pc^{-1}}{Pc(S_{wc})} \qquad \text{(Eq. 23)}$$

Behaviour Number Two: the Q&S formulation accounts for the initial time behaviour in Oil-Gas system (with Pc) during Gravity recovery mechanism however it gets slower versus time?

As discussed in the Pseudoisation section, Q&S assume the saturation front by the fracture fluid reaches the centre of the block instantly at the beginning of the invasion (Fig. 21-B). However, the gas-oil system is a special case because the displacement is vertical so the whole process is in early time until final recovery. Thus the matrix fluid in front of the saturation front will have high values of kr_o for a longer period; a promotion to a faster oil speed (Fig. 22-A). In the other hand, where the Q&S assume an end to early time at the beginning of the simulation, the K_{ro} will decrease and the Pc will increase accordingly to the semi-steady state assumption (Fig. 22-B).

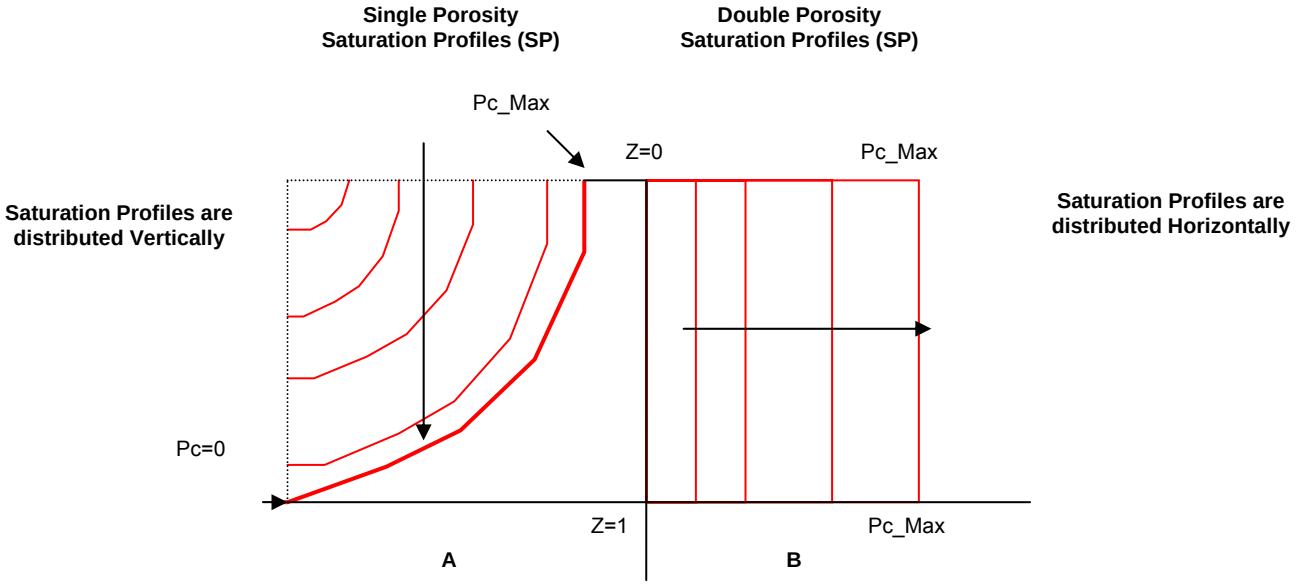

Figure 22, Saturation Profiles for (A) Fine grid single porosity and (B) dual-porosity

Behaviour Number Three: Why does the GTF drastically miss the speed recovery in Gas-Oil system with low capillary pressure?

Because the final recovery is larger, thus small end point motilities taken in delta will drastically decrease the speed of recovery. So different values need to be taken in this case as explained in Lu et al. (2006).

Transfer Function Comparison Key Points

From the previous sensitivity analysis, and comparison between the TFs we could point the following key-points out:

KZ: Kazemi
- Does not represent the gravity effect,
- Completely improper for GO systems where the only favourable driver is the gravity forces.
- It underestimates the speed of recovery.
- When capillary forces tend to trap the hydrocarbons inside the matrix blocks (WO oil-wet or mixed-wet systems), the final (maximum) recovery is underestimated, because the model stops the recovery forces as soon as Pc becomes negative for WO systems.

G&K: Gilman and Kazemi - Kazemi+GR
- Does not represent the early time recovery.
- The gravity effect is overestimated due to its presences in all of the six faces.
- When X and Y are relatively longer than Z, the TF tends to perform better; gravity effect is less.

Q&S: Quandalle and Sabathier
- Does not represent the early time recovery.
- Captures more or less the typical mixed-wet system recovery curve depending on the particular data.
- Best performer in gravity drainage.
- Is stable and gives average results comparing to the fine grid model.

GTF
- J^* and end point mobility are very sensitive where any small change in them could miss match the reference case.
- Most cases matches the early time recovery however the pace of the recovery stays at the same speed which tends to overestimate the speed of the recovery.

Commercial simulators

Almost all general purpose fluid flow simulators, like Eclipse, VIP (or Nexus), Athos, or specialised flow simulators like STARS provide a dual-medium option (dual porosity and dual permeability), where the model uses a Warre&Root-based TF.

We have only tested Eclipse and Athos (now called PumaFlow).

Eclipse

In Eclipse, three TF options are available: *KZ* (default option), *G&K* ('GRAVDR' option), and since 1998 the *Q&S* TF ('GRAVDRM'). The first one is only applicable when the gravity effects are negligible. The two other options need an integration of the Pc curves (imbibition for WO and GW systems, and drainage for GO systems). This is done automatically by the simulator with the 'INTPC' option.

We simulated our reference cases in dual-porosity, and compared the results with our own code (single-block dual-porosity model). The various options in Eclipse are in agreement with the TF formulation they are supposed to use. According to the study presented in this paper, 'GRAVDRM' and 'INTPC' options are generally recommended.

Athos

Until recently, Athos strong point was its dual-medium approach. The only TF available in Athos is *Q&S*, which was precisely developed to be implemented in this commercial simulator. The possibility to calibrate the TF via the tuning parameters for each type of term (κ_v for viscous flow term, κ_g for gravity one, and κ_c forcapillary one) is not straight forward and the improvements are limited. The use of *Q&S* TF in Athos also needs a pseudoisation of the Pc curves.

The comparison using *Q&S*, between our single-block dual-porosity calculator, Eclipse results (GRAVDRM) and Athos on our reference cases, showed very small differences.

Before new TF be implemented in new simulators, these two commercial flow simulators are acceptable. However a prior sensitivity analysis might be useful, as well as calibration to dynamic data.

Conclusions

At the core of the dual-medium approach to simulate fractured reservoirs (when appropriate) is the representation of the exchange between matrix and fracture. We presented and compared mainly two types of Warren&Root-based Transfer Functions: Kazemi and Gilman (KZ and G&K), and Quandalle and Sabathier (Q&S), plus a new type of TF called the Generalised Transfer Function – GTF - from Lu et al. (2006, 2007).

We based our investigation first on a sensitivity analysis of the main Black Oil recovery mechanisms (except diffusion), running fine-grid explicit (single-porosity) simulations of a single matrix block. Then we used these reference solutions to benchmark the main TF cited above, by running a single-matrix-block dual-porosity code (easily done in any programming language) to predict the recovery curve with respect to time (with infinitely large fracture). These tests illustrated the importance of the capillary pressure curve and representation in the TFs, the issue of capturing both early time, and late time.

While the initial Kazemi (1976) formulation has very limited validity, the most common one, Gilman and Kazemi (1983) - G&K - intends to represent the gravity drainage, but fails to be predictive for mixed-wet systems where capillary and gravity forces are in competition. The formulation proposed by Quandalle and Sabathier (1989) introduces a better representation of the gravity forces, by splitting the exchange flow between horizontal and lateral, and based on a vertical equilibrium approach (and fracture average density).

However all these WRTFs studied in this paper have the following weak points (during capillary imbibition):

- they do not represent the early time recovery effect accurately, they tend be slow;
- they do not represent the late time recovery effect accurately, they tend to be slow or fast.

We have already addressed these issues and possible improvements, confronted to Q&S and GTF results, will be presented in a coming paper.

The novel formulation (non-WRTF type) proposed by Di Donato et al. (2005), Lu et al. (2006) performs very well for early time, but needed an adjustment for mixed-wet system, which was successfully suggested by Lu et al. (2007), inspired by the Q&S formulation. The GTF formulation seems to present a good potential, but does not always represent the late time behaviour correctly. The GTF has been recently adjusted to correct the way the gravity is accounted for (Lu, 2008), but we have not tested it yet.

For the time being, the most used formulations in commercial simulators are still the WRTFs, amongst which the Q&S should be preferred for its fairly good performances (the weak point is still the representation of gravity).

Acknowledgments

We thank TOTAL Scholarship Program for their contribution. We also thank Total S.A. for authorizing the publication of this paper, and Qatar Petroleum for facilitating the finalisation of this paper. We are also grateful to Martin Blunt, and Lin Hu, and the Imperial College London ISF project team, for the stimulating exchanges.

References

Barenblatt, G.E., Zheltov, I.P., and Kochina, I.N., "Basic Concepts in the Theory of Homogeneous Liquids in Fissured Rocks", Journal of Applied Mathematical Mechanics (USSR), 1960.

Barentblatt, G. I., Entov, V. M., and Ryzhik, V. M. *Theory of Fluid Flows Through Natural Rocks*. Kluwer Academic Publishers, Dordrecht (1990).

Chang, M., "Deriving the Shape Factor of a Fractured Rock Matrix", Technical Report NIPER-696 (DE93000170), NIPER, Bartlesville OK, Sep. 1993.

Chen, J., Miller, M., Sepehrnoori, K.: " Investigations of Matrix-Fracture Transfer Flows in Dual Porosity Modelling of Naturally Fractured Reservoirs", SPE 29562, 1995.

Coats, K. H., "Implicit Compositional Simulation of Single-Porosity and Dual-Porosity Reservoirs", SPE 18427, proceedings of the SPE Symposium on Reservoir Simulation in Houston, TX, 6-8 February (1989).

Di Donato, G., Lu, H., Tavassoli, Z. and Blunt, M. J.: "Multirate transfer dual porosity modelling of gravity drainage and imbibition," SPE 93144, proceedings of the SPE Reservoir Simulation Symposium, Houston, TX, 31 January - 2 February (2005).

Garcia, M., Gouth, F., and Gosselin, O. R., "Fast and efficient modelling and conditioning of naturally fractured reservoir models using static and dynamic data", SPE-107525, proceedings of the SPE EUROPEC, London, 11-14 June, (2007)

Gilman J.R., and Kazemi, H.: "Improvement in simulation of naturally fractured reservoirs", SPE 10511, *SPEJ* **23**, 695-707 (August 1983).

Gilman, J.R., "An Efficient Finite-Difference Method for Simulating Phase Segregation in Matrix Blocks in Double-Porosity Reservoirs", published in SPE RE, July 1986.

Hagoort, J.: "Oil Recovery by Gravity Drainage." SPEJ 20. 139-150 (June 1980).

Ishimoto, K.:"Improved Matrix, Fracture Fluid Transfer Function in Dual Porosity Models", SPE 17599, 1988.

Kazemi, H., Merrill, L., Porterfield, K. and Zeman P., "Numerical Simulation of Water-Oil Flow in Naturally Fractured Reservoirs", SPE 5719, SPEJ 16, 318-326 (December 1976).

Lim, K.T. and Aziz, K., "Matrix-Fracture Transfer Shape Factors for Dual Porosity Simulators", Journal of Petroleum Science and Engineering, 1995.

Lu H., Di Donato G., and Blunt M. J., "General Transfer Functions for Multiphase Flow", SPE 102542, proceedings of the SPE Annual Meeting, San Antonio, Texas, 24 – 27 September (2006)

Lu H., and Blunt M. J., "General Fracture/Matrix Transfer Functions for Mixed-Wet Systems", SPE 107007, proceedings of the SPE EUROPEC, London, UK, 11-14 June (2007).

Lu, H., "Investigation of Recovery Mechanisms in Fractured Reservoirs", PhD Thesis, Imperial College London, Royal School of Mines, Department of Earth Science and Engineering, February 2008.

Quandalle, P. , Sabathier, J. C., "Typical Features of a Multipurpose Reservoir Simulator", SPERE, November 1989.

Ramirez, B., Kazemi, H., Al-kobaisi, M., Ozakan, E. and Atan, S. : 'A Critical Review for Proper Use of Water-Oil-Gas Transfer Functions in Dual-Porosity Naturally Fractured Reservoirs – Part 1' SPE 109821.

Sarma, P., "New Transfer Functions for Simulation of Naturally Fractured Reservoirs with Dual-Porosity Models." MS thesis. Stanford, California: Stanford U., 2003.

Sonier, F.; Souillard, P., and Blaskovich, F.T., « Numerical Simulation of Naturally Fractured Reservoirs », SPE 15627, SPE Res. Eng. 1114-1122 (November 1988).

Warren, J.E. and Root, P.J., "The Behavior of Naturally Fractured Reservoirs", SPEJ. 3, 245-255, (Sept. 1963)

Zhang, X., Morrow, N. R., and Ma, S.: "Experimental Verification of a Modified Scaling Group for Spontaneous Imbibition," *SPERE*, **11**, 280-285 (1996).

Zimmerman, R. W., Chen, G., Hadgu, T. and Bodvarsson, G. S.:"A Numerical Dual-Porosity Model With Semi-analytical Treatment of Fracture/Matrix Flow," *Water Resources Research*, **29**(7), 2127-2137 (1993).

Nomenclature

a	representative height
A	area, m2
c	component concentration, dimensionless
D	diffusion coefficient, m^2s^{-1}
F	weighting function, dimensionless
g	gravity acceleration, ms^{-2}
H, h	height, m
J*	dimensionless capillary pressure
K	permeability, mD
kr	relative permeability, dimensionless
L, l	length, m
L_c	characteristic length
M	mass per unit volume, kgm^{-3}
P	pressure, Pa
Pc	capillary pressure, Pa
S	saturation, dimensionless
S*	max. saturation of invading fluid, dimensionless
T	volume transfer function for phase, s^{-1}
t	time, s
u	velocity, ms-1
V	block volume, m3
Γ	mass transfer term for component, $kg.m^{-3}.s^{-1}$
δ	rate in displacement transfer (GTF), s^{-1}
κ	tuning parameters in Q&S, dimensionless
ρ*	average density in Q&S, kgm^{-3}
ρ	density, kgm^{-3}
σ	shape factor, m^{-2}
ς	interfacial tension in Pc equation, $N.m^{-1}$
ε	small convergence parameter, dimensionless
ϕ	porosity, %
μ	viscosity, Pa.s
λ	phase mobility $Pa^{-1}.s^{-1}$
ψ	pressure potential, Pa

Subscripts

c	capillary force
d	diffusion
D	dimensionless
f	fracture (for porosity, permeability)
g	gravity force
g	gas phase
hor	horizontal
i	initial
j	direction of flows (matrix-fracture)
m	matrix (for porosity, permeability)
o	oil phase
p	transfer function direction; Q&S.
e	fluid expansion
s	fluid displacement
v	viscous force
ver	vertical.
w	water phase
x, y, z	direction
α, β	phase label
ξ	black oil pseudo-component

Superscripts

d	domain; matrix or fracture.
f	fracture
H	horizontal
m	matrix
V	vertical
*	End-point
-,+	direction

Appendix A: Base Case parameters

Property	Base Case
Initial Matrix Pressure (atm)	400
Initial Fracture Pressure (atm)	400
Water Density at Initial matrix pressure (g/cm3)	1.01
Water compressibility (1/atm)	4.50E-05
Water viscosity (Pa.s)	0.00022
Block width-x (cm)	79
Block length-y (cm)	79
Block height-z (cm)	800
Block Volume (cm3)	5.0E+06

Table 3, Base Case ALL Systems

Property	Base Case
Initial Matrix Water Saturation	0.1
Initial Fracture Water Saturation	1
Residual Oil Saturation	0.2
K_{rw} @ S_{or}	0.8
K_{ro} @ S_{wc}	1
Max Capillary Pressure @ Sw =0.1 (atm)	0.2
Water Saturation @ Pc=0	0.5
Water Saturation @ Pc = $\Delta\rho_{ow}gh$	0.8
Oil Density at initial matrix pressure (g/cm3)	0.65
Oil compressibility (1/atm)	4.50E-04
Oil Viscosity (Pa.s)	0.0005

Table 4, Base Case Oil-Water System

Property	Base Case
Initial Matrix Water Saturation	0.1
Initial Matrix Gas Saturation	0
Initial Fracture Water Saturation	0
Initial Fracture Gas Saturation	1
Residual Oil Saturation	0.2
K_{rg} @ S_{or}	0.75
K_{ro} @ S_{gc}	1
Max Capillary Pressure @ Sg =1.0 (atm)	1
Oil Density at initial matrix pressure (g/cm3)	0.65
Gas Density at intial matrix pressure (g/cm3)	0.001
Oil compressibility (1/atm)	4.50E-04
Gas compressibility (1/am)	2.50E-06
Rock Compressibility (1atm)	-
Oil Viscosity (Pa.s)	5.00E-04
Gas Viscosity (Pa.s)	4.70E-05

Table 5, Base Case Oil-Gas System

Property	Base Case
Initial Matrix Water Saturation	0.4
Initial Fracture Water Saturation	1
Residual Gas Saturation	0.305
K_{rw} @ S_{gr}	1
K_{rg} @ S_{wc}	1
Max Capillary Pressure @ Sw =0.4 (atm)	7.5
Water Saturation @ Pc=0	0.695
Gas Density at initial matrix pressure (g/cm3)	0.001
Gas compressibility (1/atm)	2.50E-03
Gas Viscosity (Pa.s)	4.78E-05

Table 6, Base Case Gas-Water System

Appendix B: Base Case kr and Pc

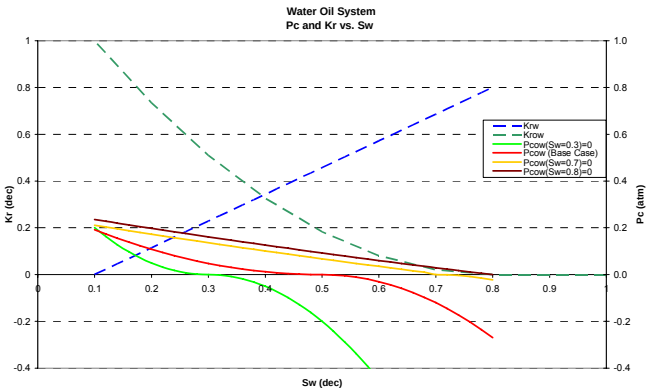

Figure 23, Oil Water System Base Case Pc and Kr curves

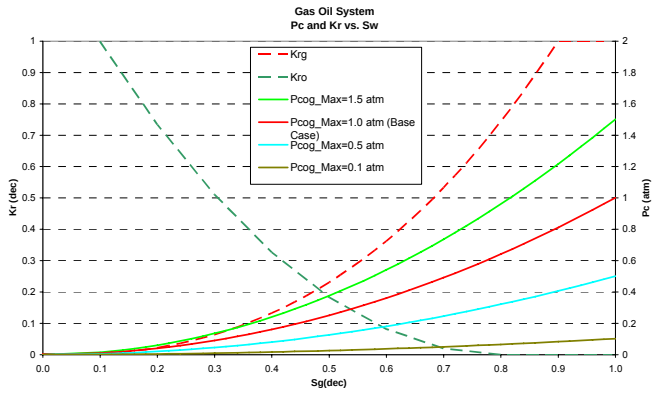

Figure 24, Gas-Oil System base case Pc and Kr

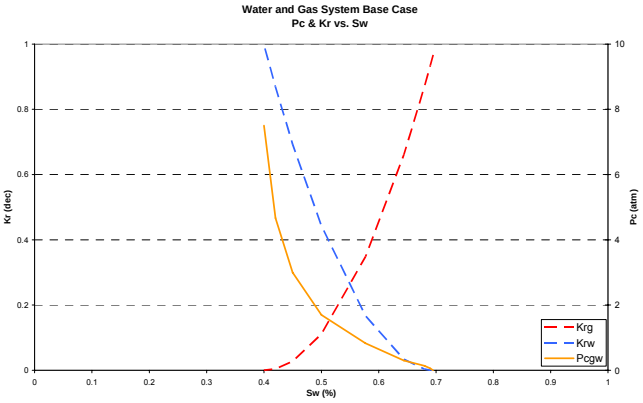

Figure 25, Gas-Water System base case Pc and Kr

Appendix C Kazemi transfer function formulation and simulation

Here we derive the Kazemi transfer function. Under the assumption of overlapped continuum between the matrix and the fracture cells, the flow function of the six faces of a matrix cell can be derived by the following (Darcy's law) for each face.

$$u_{\alpha,z+} = \lambda_\alpha K_m (\Psi_\alpha^m - \Psi_{\alpha,z+}^f) \frac{l_x l_y}{\frac{l_z}{2}} \quad \text{(Eq. C1)}$$

$$u_{\alpha,z-} = \lambda_\alpha K_m (\Psi_\alpha^m - \Psi_{\alpha,z-}^f) \frac{l_x l_y}{\frac{l_z}{2}} \quad \text{(Eq. C2)}$$

$$u_{\alpha,x+} = \lambda_\alpha K_m (\Psi_\alpha^m - \Psi_{\alpha,x+}^f) \frac{l_z l_y}{\frac{l_x}{2}} \quad \text{(Eq. C3)}$$

$$u_{\alpha,x-} = \lambda_\alpha K_m (\Psi_\alpha^m - \Psi_{\alpha,x-}^f) \frac{l_z l_y}{\frac{l_x}{2}} \quad \text{(Eq. C4)}$$

$$u_{\alpha,y+} = \lambda_\alpha K_m (\Psi_\alpha^m - \Psi_{\alpha,y+}^f) \frac{l_z l_x}{\frac{l_y}{2}} \quad \text{(Eq. C5)}$$

$$u_{\alpha,y-} = \lambda_\alpha K_m (\Psi_\alpha^m - \Psi_{\alpha,y-}^f) \frac{l_z l_x}{\frac{l_y}{2}} \quad \text{(Eq. C6)}$$

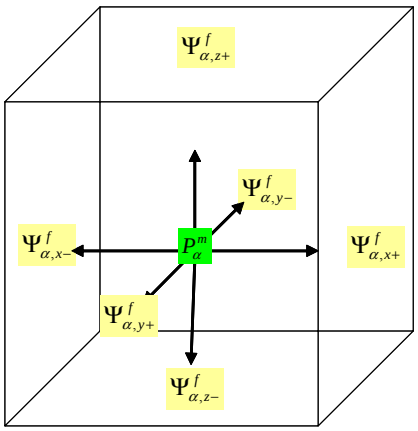

Fig. 26, Pressure potentials in matrix cell

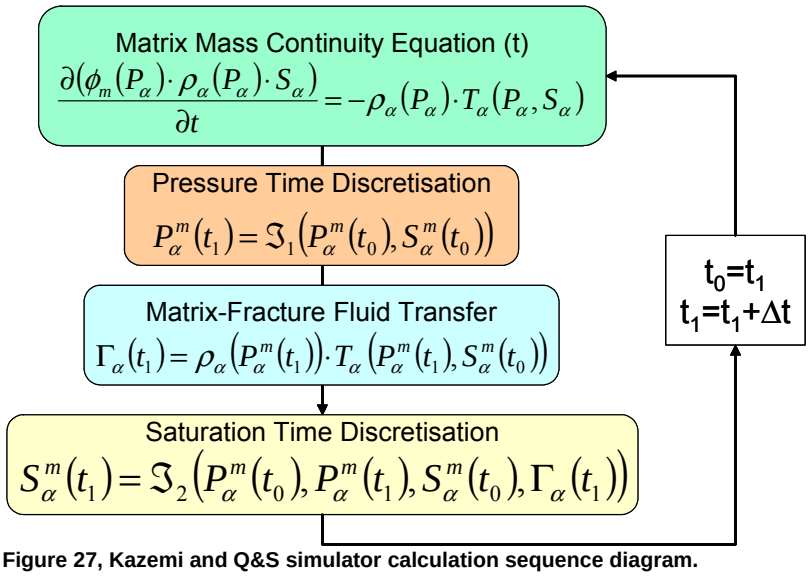

Figure 27, Kazemi and Q&S simulator calculation sequence diagram.

Then we add the six equations and divide them by the block volume. Taking the same mobility, permeability and fracture potential on all the six faces (assumed by Kazemi et al.)

$$\Gamma_\alpha = 4\left(\frac{1}{l_x^2}+\frac{1}{l_y^2}+\frac{1}{l_z^2}\right)\lambda_\alpha K_m\left(\Psi_\alpha^m-\Psi_\alpha^f\right)=\sigma\lambda_\alpha K_m\left(P_\alpha^m-P_\alpha^f\right) \qquad \text{(Eq. C7)}$$

Fig. 27 shows the calculation sequence in the in house zero dimensional double porosity simulator for the Kazemi and Q&S transfer functions.

Appendix D: Q&S transfer function formulation and simulation

Here we derive the Q&S transfer function. Under the assumption of overlapped continuum between the matrix and the fracture cells, the flow function of the six faces of a matrix cell can be derived by the following (Darcy's law) for each face. However, in the Q&S formulation, each face holds its mobility, permeability and face potential; while in Kazemi they are assumed similar. First, we will define the potential at each face in the matrix and the fracture, please refer to Fig. 28 for illustration.

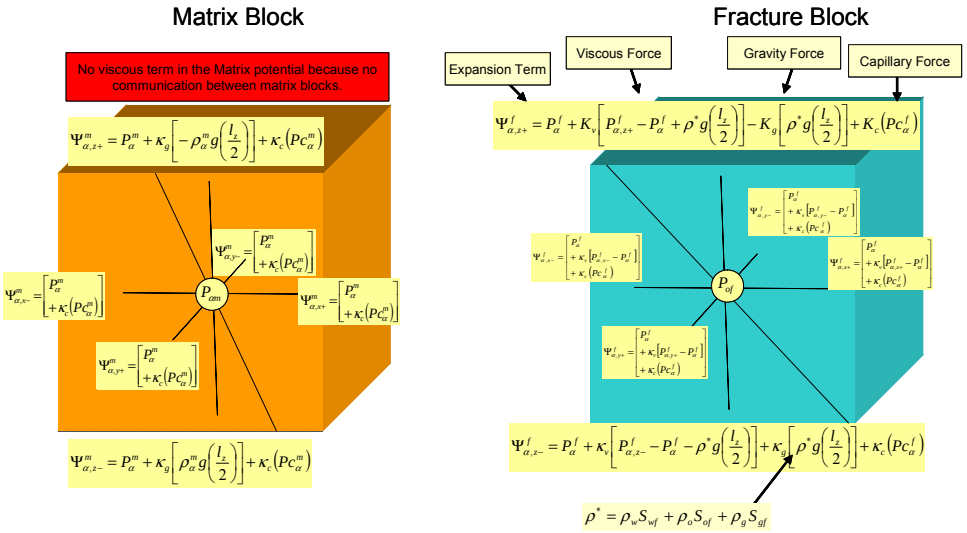

Figure 28: Q&S face potentials in the matrix and fracture cells

Then, from the above potentials we can define the transfer function for each face,

$$T_{\alpha z}^{+}=2\sigma_z\lambda_\alpha(M,F)_{z^+}K_{zm}\left(P_\alpha^m-P_\alpha^f-\kappa_v\left[P_{\alpha,z+}^f-P_\alpha^f+\rho^*g\left(\frac{l_z}{2}\right)\right]-\kappa_g\left[\left(\rho_\alpha^m-\rho^*\right)g\left(\frac{l_z}{2}\right)\right]+\kappa_c\left(Pc_\alpha^m-Pc_\alpha^f\right)\right) \qquad \text{(Eq. D1)}$$

$$T_{\alpha z}^{-}=2\sigma_z\lambda_\alpha(M,F)_{z^-}K_{zm}\left(P_\alpha^m-P_\alpha^f-\kappa_v\left[P_{\alpha,z-}^f-P_\alpha^f-\rho^*g\left(\frac{l_z}{2}\right)\right]+\kappa_g\left[\left(\rho_\alpha^m-\rho^*\right)g\left(\frac{l_z}{2}\right)\right]+\kappa_c\left(Pc_\alpha^m-Pc_\alpha^f\right)\right) \qquad \text{(Eq. D2)}$$

$$T_{\alpha x}^{+}=2\sigma_x\lambda_\alpha(M,F)_{x^+}K_{xm}\left(P_\alpha^m-P_\alpha^f-\kappa_v\left[P_{\alpha,x+}^f-P_\alpha^f\right]+\kappa_c\left(Pc_\alpha^m-Pc_\alpha^f\right)\right) \qquad \text{(Eq. D3)}$$

$$T_{\alpha x}^{-}=2\sigma_x\lambda_\alpha(M,F)_{x^-}K_{xm}\left(P_\alpha^m-P_\alpha^f-\kappa_v\left[P_{\alpha,x-}^f-P_\alpha^f\right]+\kappa_c\left(Pc_\alpha^m-Pc_\alpha^f\right)\right) \qquad \text{(Eq. D4)}$$

$$T_{\alpha y}^{-}=2\sigma_y\lambda_\alpha(M,F)_{y^-}K_{ym}\left(P_\alpha^m-P_\alpha^f-\kappa_v\left[P_{\alpha,y-}^f-P_\alpha^f\right]+\kappa_c\left(Pc_\alpha^m-Pc_\alpha^f\right)\right) \qquad \text{(Eq. D5)}$$

$$T_{\alpha y}^{+}=2\sigma_y\lambda_\alpha(M,F)_{y^+}K_{ym}\left(P_\alpha^m-P_\alpha^f-\kappa_v\left[P_{\alpha,y+}^f-P_\alpha^f\right]+\kappa_c\left(Pc_\alpha^m-Pc_\alpha^f\right)\right) \qquad \text{(Eq. D6)}$$

Finally when we add them we get to equation (Eq. D7).

$$T_\alpha=\begin{bmatrix}2\sigma_z\lambda_\alpha(M,F)_{z^+}K_{zm}\left(P_\alpha^m-P_\alpha^f-\kappa_v\left[P_{\alpha,z+}^f-P_\alpha^f+\rho^*g\left(\frac{l_z}{2}\right)\right]+\kappa_c\left(\left(Pc_\alpha^m-Pc_\alpha^f\right)\right)-\kappa_g\left[\left(\rho_\alpha^m-\rho^*\right)g\left(\frac{l_z}{2}\right)\right]\right)\\ +2\sigma_z\lambda_\alpha(M,F)_{z^-}K_{zm}\left(P_\alpha^m-P_\alpha^f-\kappa_v\left[P_{\alpha,z-}^f-P_\alpha^f-\rho^*g\left(\frac{l_z}{2}\right)\right]+\kappa_c\left(\left(Pc_\alpha^m-Pc_\alpha^f\right)\right)+\kappa_g\left[\left(\rho_\alpha^m-\rho^*\right)g\left(\frac{l_z}{2}\right)\right]\right)\\ +2\sigma_x\lambda_\alpha(M,F)_{x^+}K_{xm}\left(P_\alpha^m-P_\alpha^f-\kappa_v\left[P_{\alpha,x+}^f-P_\alpha^f\right]+\kappa_c\left(Pc_\alpha^m-Pc_\alpha^f\right)\right)\\ +2\sigma_x\lambda_\alpha(M,F)_{x^-}K_{xm}\left(P_\alpha^m-P_\alpha^f-\kappa_v\left[P_{\alpha,x-}^f-P_\alpha^f\right]+\kappa_c\left(Pc_\alpha^m-Pc_\alpha^f\right)\right)\\ +2\sigma_y\lambda_\alpha(M,F)_{y^+}K_{ym}\left(P_\alpha^m-P_\alpha^f-\kappa_v\left[P_{\alpha,y+}^f-P_\alpha^f\right]+\kappa_c\left(Pc_\alpha^m-Pc_\alpha^f\right)\right)\\ +2\sigma_y\lambda_\alpha(M,F)_{y^-}K_{ym}\left(P_\alpha^m-P_\alpha^f-\kappa_v\left[P_{\alpha,y-}^f-P_\alpha^f\right]+\kappa_c\left(Pc_\alpha^m-Pc_\alpha^f\right)\right)\end{bmatrix} \qquad \text{(Eq. D7)}$$

The simulation calculation sequence is the same than Kazemi and illustrated in Fig. 27.